John D. O'Toole
Vice President

Consolidated Edison Company of New York, Inc.
4 Irving Place, New York, NY 10003
Telephone (212) 460-2533

Letter No. 81-126
July 28, 1981

RE: Indian Point Unit No. 2
Docket No. 50-247

RECEIVED
AUG 04 1981
U.S. NUCLEAR REGULATORY COMMISSION

Director of Nuclear Reactor Regulation
U. S. Nuclear Regulatory Commission
Washington, D.C. 20555

ATTN: Mr. Steven A. Varga, Chief
Operating Reactors Branch No. 1
Division of Licensing

Dear Mr. Varga:

This is in response to your June 8, 1981 letter requesting additional information on the proposed expansion of the capacity of the IP2 spent fuel pool. Enclosure 1 contains our responses to the questions contained in your letter.

Our schedule for installation of the higher capacity spent fuel storage racks requires that NRC review actions be completed by Oct. 1, 1981. This schedule will permit the modifications to be carried out before the arrival of the next reload batch of fuel, at which time the existing storage facility will no longer allow full core discharge without the planned expansion. Your cooperation is resepctfully requested.

Should you or your staff have any questions, please contact us.

Very truly yours,

John D. O'Toole

Enclosure

A001
S.1

8108050155 810728
PDR ADOCK 05000247
P PDR

1 MR. PIGOTT: Is the witness now tendered for cross
2 examination?
3 MR. WHARTON: Yes.
4 JUDGE KELLEY: Yes, he is.
5 CROSS EXAMINATION
6 BY MR. PIGOTT:
7 Q Mr. Legg, turning to your testimony. We may as
8 well take it as you go through it. Section two, Northward
9 Continuation of the Agua Blanca Fault.
10 Did you draft this testimony yourself or was it done
11 under your supervision and direction?
12 A I drafted this testimony myself.
13 Q In the first paragraph, you get to the -- at
14 the bottom of that first paragraph in section two. You have
15 a couple of questions posed. One is, "does the San Clemente
16 fault connect with the Agua Blanca fault as suggested by
17 Allen." That's Clarence Allen, I assume?
18 A Yes, sir.
19 Q And"what is the lateral extent and character
20 of these faults." First of all, as I understand your
21 testimony, you've determined that Clarence Allen was wrong.
22 Is that correct? That Agua Blanca does not connect with the
23 San Clemente?
24 A Yes, sir, that is what I have determined.
25 Q These questions were posed for what purpose?

50-247

RESPONSE TO NRC QUESTIONS
ON
SPENT FUEL POOL EXPANSION

Received wth ltr dtd 7/28/81

— NOTICE —

THE ATTACHED FILES ARE OFFICIAL RECORDS OF THE DIVISION OF DOCUMENT CONTROL. THEY HAVE BEEN CHARGED TO YOU FOR A LIMITED TIME PERIOD AND MUST BE RETURNED TO THE RECORDS FACILITY BRANCH 016. PLEASE DO NOT SEND DOCUMENTS CHARGED OUT THROUGH THE MAIL. REMOVAL OF ANY PAGE(S) FROM DOCUMENT FOR REPRODUCTION MUST BE REFERRED TO FILE PERSONNEL.

Docket # 50-247
Control #8108050155
Date 7-28-81 of Document
REGULATORY DOCKET FILE

DEADLINE RETURN DATE

REGULATORY DOCKET FILE COPY

RECORDS FACILITY BRANCH

ENCLOSURE 1
RESPONSE TO NRC QUESTIONS ON
SPENT FUEL POOL EXPANSION, INDIAN POINT-2

Response 1: The borated stainless steel sheets used in the Indian Point-2 racks are modified Type 304 stainless steel with boron distributed uniformly throughout its volume. Boron is introduced as an iron boron compound (FeB) into the molten stainless steel mix in an electric furnace. The boron uniformly distributed throughout the molten metal. The metal is then cast into ingots and hot-rolled on conventional rolling mills. It is subsequently annealed and cold rolled to size on conventional steel mill equipment. The isotopic boron ratios are about 18% B-10 and 82% B-11. The nominal boron concentration in the plate is 1.1 w/o and the minimum boron concentration is 1.0 w/o as reported on the supplier's Certificate of Test forms.

Response 2: A coupon surveillance program will be used to assure that boron remains in the stainless steel plates throughout the lifetime of the racks. The baseline data will provide the necessary information/characteristics for later comparison after the coupons have been exposed to the pool environment.

REGULATORY DOCKET FILE COPY

Response 3: Boron self-shielding was taken into account in the sensitivitiy study using blackness theory (Reference 1).

Response 4: The uncertainties in KENO-IV criticality calculation can be divided into two categories:

1. Uncertainty due to the statistical nature of Monte Carlo calculations, (the variance of k_{eff} values over many generations).
2. Uncertainty due to bias in the calculation techniques.

The variance of k_{eff} values for the many neutron generations is directly determined in the KENO-IV calculations. Its magnitude can be reduced by increasing the number of neutrons tracked. For fuel rack criticality calculations, the number of neutrons tracked is selected to reduce the variance to less than 1%. This variance is accounted for in the final result by statistically adding it to variations due to other normal varations in k_{eff}. The 0.006 statistical uncertainty report for Indian Point 2 was obtained directly from the KENO-IV output.

---

1. A. Radkowski Naval Reactor Physics Handbook, Volume 1, Naval Reactors Division of Reactor Development, U.S.A.E.C., 1964

The second class of uncertainty is accounted for by benchmarking the calculational method against experimental results. In the benchmarking process, the calculation method is used to determine the criticality value(k_{eff}) for a critical experiment configuration. The difference between the calculated criticality value and the experimental value is identified as the calculational bias. Once determined, this bias can be applied to other calculated results obtained for similar configurations to improve the degree of calculational accuracy. If the calculated criticality value found during benchmarking is less than the experimental value, the bias is added to other calculation results to ensure accurate values consistent with experimental results. Conversely, if the calculated criticality value is greater than the experimental value, it is appropriate to subtract the bias from the other calculated results to improve the accuracy of the criticality determination. A variety of Benchmarking configurations were reviewed by NES, including critical experiments

performed by Babcock & Wilcox [1,2,3] (note: Ref. 1 is a summary of Ref. 3). Battelle Northwest Laboratories[4] and Allis Chalmers[5]. No one critical experiment contained all the elements present in a fuel storage rack. It became necessary to perform several calculations to achieve an understanding of the accuracy of KENO-IV for high density fuel storage rack configurations.

1. G. Hoovler, et al, Critical Experiments Supporting Close Proximity Water Storage at Power Reactor Fuel, Nuclear Technology, Vo. 51, Dec. 1980, p. 217.

2. Bromley, W.D., Olszewski, L. S. Safety Calculations and Benchmarking of Babcock and Wilcox Designed Close Spaced Fuel Storage Racks, Nuclear Technology, Vol. 41, Mid-December 1978, p. 346.

3. M. N. Baldwin, et al, Criticaltiy Experiments Supporting Close Proximity Storage of Power REactor Fuel. Summary Report, BAW-1484-7, Babcock and Wilcox, Lynchburgh, Va. July 1979.

4. Bierman, S. R. Durst, B. M. Critical Separation Between Clusters of 4.29 wt% 235U Enriched UO2 Rods in Water with Fixed Neutron Poisons, May 1978, NUREG/Gr-0073-RC.

5. NES 81A0260, "Criticality Analysis of the Atcor Vandenburgh Cask", R. J. Weader, February, 1975.

We concur that k_{eff} values obtained by KENO-IV in (Reference 1, previous page) for the specific geometry configuration of large assembly separations with no steel or absorbing media present between assemblies are not always greater than experimental values. However, for other configurations representative of the fuel rack environment, such as lattices containing internal water gaps, internal stainless steel poison plates and internal boron poison plates, Bromley and Olszewski (Reference 2 on previous page) have reported higher values than experimental results. NES has consistently been able to achieve similar results in benchmarking studies. It should be reiterated that in order to ensure adequate conservatism, NES has not taken credit for any overprediction of k_{eff} in the Indian Point 2 rack nuclear analysis.

Response 5: Cell pitch, cell wall thickness and cell I.D. were treated as independent variables to account for individual effects on k_{eff} due to material manufacturing and rack fabrication and assembly tolerances. These variables are indeed independent of each other since they are determined by individual measurements made during the fabrication process. Although it would be possible to treat these variables as aspects of the metal/water ratio for analysis purposes, it is nevertheless necessary to establish the individual variables that make up that ratio to establish the correspondence between design dimensional tolerances that may be allowed during actual fabrication and their effects on k_{eff}. The treatment of cell wall thickness in our sensitivity analysis was broken down into three areas:

1. Variation of the can wall thickness (SS 304)
2. Variation of the thickness of the borated stainless steel (BSS) sheet (at a constant boron concentration).
3. Variation of the boron concentration within the borated stainless steel (at a constant BSS thickness).

In this manner, the elements of wall thickness were isolated and treated independently. Clearly an increase in either stainless steel wall thickness or borated stainless steel thickness will displace some moderator. Displacement of moderator is effectively similar to a pitch change. A 0.0025 inch (the maximum variation allowed) increase in stainless steel wall thickness while maintaining a constant cell I.D. resulted in a net increase in k_{eff} of 0.002. The change in k_{eff} predicted from pitch variations is 0.0004. Thus the isolated effect of the stainless steel is a decrease in k_{eff} of 0.0002.

We must conclude that the displacement of moderator has a dominant effect on k_{eff} for this variation.

A 0.004-inch decrease in borated stainless steel thickness (the maximum decrease allowed) resulted in a net increase in k_{eff} of 0.00128. The change in k_{eff} predicted from pitch calculation to account for displaced moderator is -0.00065. We conclude therefore that the displacement of moderator is a negligible contribution to this variation.

The variation of boron concentration within the borated stainless steel does not result in a displacement of moderator.

To summarize the normal variation considered in the analysis:

Variation	Δk_{eff}
Eccentric positioning (all due to moderator displacement)	0.0040
Enrichment variation	0.0000 (maximum used)
Minimum cell pitch (-1/64") (all due to moderator displacement)	0.0013
Maximum stainless steel can wall thickness (+0.0025")	
Δk due to moderator displacement	0.0004
Δk due to increase in steel thickness alone	-0.0002
net effect of variation	0.0002
Minimum borated stainless steel thickness (-0.004")	
Δk due to moderator displacement	-0.00065
Δk due to borated stainless steel thickness reduction	+0.00183
net effect of variation	0.0013
Minimum poison concentration (-0.1w/o)	0.0040
Maximum cell Inner Diameter	0.0060

Response 6: The Quality Assurance Programs consist of a multi-tier arrangement whereby the boron stainless steel (the poison) supplier, Carpenter Technology, the design engineer, Nuclear Energy Services, and the licensed operator, Con Edison, all have approved Quality Assurance Programs.

Con Edison's Quality Assurance requirements have been imposed and incorporated into NES's Quality Assurance Program Plan (QAPP). In addition, this QAPP has been reviewed and approved by Con Edison. Similarly, NES has imposed this QAPP on Carpenter Technology. Moreover, Consolidated Edison has had previous satisfactory QA experience with Carpenter who were suppliers for our first spent fuel rack replacement in 1975. Carpenter Technology has, in addition to a Quality Assurance Program manual, a Quality Verification Plan containing such details as time and temperature for each operation set forth in a step by step fashion to assure adequate controls on boron concentration. The boron concentration in the steel is determined by chemical analysis and documented on supplier's Certificate of Test forms. These tests are performed for each individual heat and are certified to satisfy a 95/95 confidence level. The results are also confirmed by Consolidated Edison on randomly selected heats. NES has been assigned the prime responsibility for the surveillance of the poison steel manufacture for Consolidated Edison. To assist their inspector, NES developed a specification for the "Fabrication and Inspection of the Borated Stainless Steel" material which has

been reviewed and approved by Consolidated Edison. This Quality Assurance document covers chemistry (i.e. boron concentration) as well as, dimensions, mechanical properties, cleanliness, packaging, shipping, identification and documentation of the poison material.

Response 7a: The expansion modification of the spent fuel pool at Indian Point Unit 2 will require the load identified in Table 1A and 1B to come in close proximity to spent fuel.

The travel paths and sequence which will be used in removing and installing spent fuel storage racks are shown on Figures 1 through 6. A minimum horizontal spacing of three empty storage locations would be maintained between the lifted racks and the stored fuel. Existing racks Nos. 1,2,4 and 5 would be lifted horizontally clearing all existing racks and with a minimum horizontal distrance of five storage locations from stored fuel. All other fuel rack movements would clear at least one empty rack space.

The step by step procedure of rack installation and removal sequence is as follows:

1. Install the handling tool support rack on the south wall in the cask handling area.
2. Transfer the handling tools from their present storage position along the south wall of the pool to the new support racks. Remove the existing handling tool brackets from the south personnel handrail.
3. Transfer fuel to fully fill existing racks 6 through 10 (235 assemblies), two westernmost rows of existing racks 4 and 5 (26 assemblies), and seven locations in the southwest corner of existing rack 3, as shown in Figure 1.
4. Remove the I-beam from the northeast corner of the pool, and the light poles and support brackets from the east wall.
5. Remove the failed fuel rack and existing rack 1 by lifting them straight up and over the south wall of the pool.
6. Remove existing rack 2 by lifting it to clear its support pins, then moving it horizontally south along the east wall to a position adjacent to the new fuel elevator, and lifting it up and over the south wall.
7. Install modified light pole brackets on the east wall.
8. Install rack support plates, Types 12 and 19.
9. Install new rack 1 by lowering it into the pool adjacent to the east wall and the new fuel elevator to a position just above the elevation of existing rack 5, then moving it horizontally north along the wall and down into position.
10. Transfer 13 assemblies from existing rack 3 and north end of existing rack 4 to northernmost rows of new rack 1. Refer to Figure 2.

11. Remove existing rack 3 by lifting to clear its support pins, moving horizontally to the east wall, lifting above the level of existing rack 4, moving horizontally south to the new fuel elevator and lifting straight up and over the south wall.

Note: Rack 3 will straddle two empty rows of racks 4 and 5, clearing stored fuel by a minimum of three empty storage rows.

12. Install rack support plates, Types 13 and 14.

13. Install new rack 2 by following the same load path as in step 9 above.

14. Transfer the remaining fuel in existing racks 4 and 5, and the two easternmost rows of fuel in racks 6,7 and 8 to new racks 1 and 2. Refer to Figure 3.

15. Remove existing racks 4 and 5 by lifting them to clear pins, moving horizontally to the east wall, lifting them straight up and over the south wall.

16. Install rack support plates, Types 10, 15 through 18, and 20.

17. Install new rack 3.

18. Attach the new failed fuel rack to new rack 4 and install them in the pool as a unit.

19. Transfer fuel from existing racks 7,8 and 10, to new racks 2 and 3. Refer to Fig. 4.

20. Remove, in sequence, existing racks 8, 7, and 10. Lift racks 7 and 10 to clear pins and move them horizontally until adjacent to the south wall before lifting them out of pool.

21. Remove the seismic restraint bracket, channel (ladder) brackets, light poles and support brackets from the south wall.

22. Reinstall modified light pole fixtures and brackets on south wall.
23. Install guard support plates on new racks 5,8, 10 and 12, and guard angles on racks 5 and 8.
24. Install new racks 7 and 10.
25. Transfer all fuel from existing racks 6 and 9 to new racks 3 and 4. Refer to Figure 5.
26. Reinstall light pole fixtures on modified brackets on east wall.
27. Remove existing racks 9 and 6 from the pool.
28. Remove the seismic bracket, light poles, and support brackets from the west wall.
29. Reinstall modified light pole fixtures and brackets on west wall.
30. Install support plates, Types 1 and 7.
31. Install, in order, new racks 11,12,6,9,5 and 8. Refer to Figure 6.
32. Install guard angles on racks 10 and 12.

TABLE 1A
INDIAN POINT UNIT 2
ITEMS REMOVED FROM SPENT FUEL POOL

ITEM	TIMES HANDLED (PROJECTED)	APPROX. WEIGHT (LBS)	APPROX. SIZE (INCHES)
Old Rack 1 & Handling Tool	1	40,000	156 x 72 x 165
Old Rack 2 & Handling Tool	1	40,000	156 x 72 x 165
Old Rack 3 & Handling Tool	1	28,000	102 x102 x 165
Old Rack 4 & Handling Tool	1	28,000	102 x102 x 165
Old Rack 5 & Handling Tool	1	28,000	102 x102 x 165
Old Rack 6 & Handling Tool	1	28,000	102 x102 x 165
Old Rack 7 & Handling Tool	1	28,000	102 x102 x 165
Old Rack 8 & Handling Tool	1	28,000	102 x102 x 165
Old Rack 9 & Handling Tool	1	28,000	102 x102 x 165
Old Rack 10 & Handling Tool	1	28,000	102 x102 x 165
Old Failed Fuel Rack & Handling Tool	1	10,000	24" x 60" x 165"
"I" Beam	1	500 (max)	84" long
2 Seismic Brackets	1 (each)	100 (max)	20" x 20" x 20"
7 Light Fixtures	1 (each)	200 ea. (max)	20" x 14" x 12"

TABLE 1B
INDIAN POINT UNIT 2
ITEMS INSTALLED IN SPENT FUEL POOL

ITEM	TIMES HANDLED (PROJECTED)	APPROX. WEIGHT (LBS)	APPROX. SIZE (INCHES)
New Rack 1 & Handling Tool	1	26300	183 x 88 x 88
New Rack 2 & Handling Tool	1	26300	183 x 88 x 88
New Rack 3 & Handling Tool	1	32000	183 x 88 x110
New Rack 4 & Handling Tool	1	32000	183 x 88 x110
New Rack 5 & Handling Tool	1	38800	183 x110 x110
New Rack 6 & Handling Tool	1	38800	183 x110 x110
New Rack 7 & Handling Tool	1	32000	183 x 88 x110
New Rack 8 & Handling Tool	1	32000	183 x 88 x110
New Rack 9 & Handling Tool	1	32000	183 x 88 x110
New Rack 10 & Handling Tool	1	29300	183 x 99 x 88
New Rack 11 & Handling Tool	1	35400	183 x 98 x110
New Rack 12 & Handling Tool	1	35400	183 x 98 x110
21 Support Plates	1 (ea.)	500 ea. (max)	38 x 26 x 3¼ ea. (max)
New Failed Fuel Rack & Handling Tool	1	4000	60 x148 x 21
Leveling Wrenches & Lifting Tool	100	180	340 x 11 x 6
7 Light Fixtures	1 (ea.)	200 ea. (max)	20"x 14"x 12"
Rack Templates	12	1050	20"x110"x110"

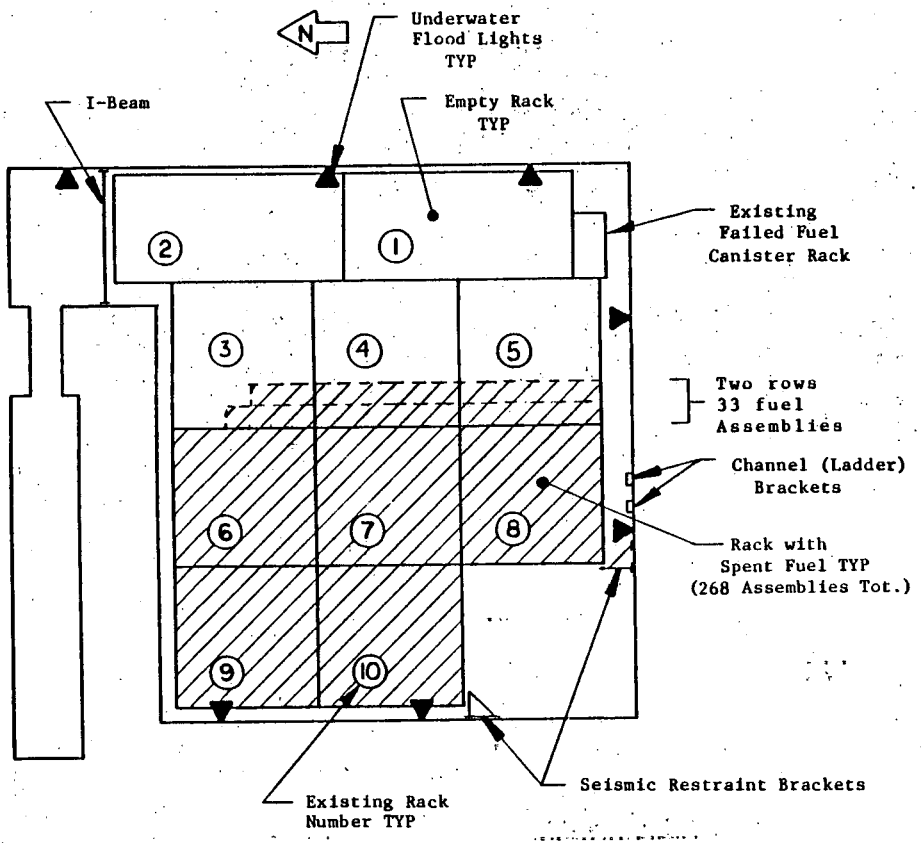

FIGURE 1
FUEL RACK INSTALLATION SEQUENCE

Existing Rack Arrangement

NUCLEAR ENERGY SERVICES, INC.
DOCUMENT NO. 80A3501
PAGE ____ OF ____

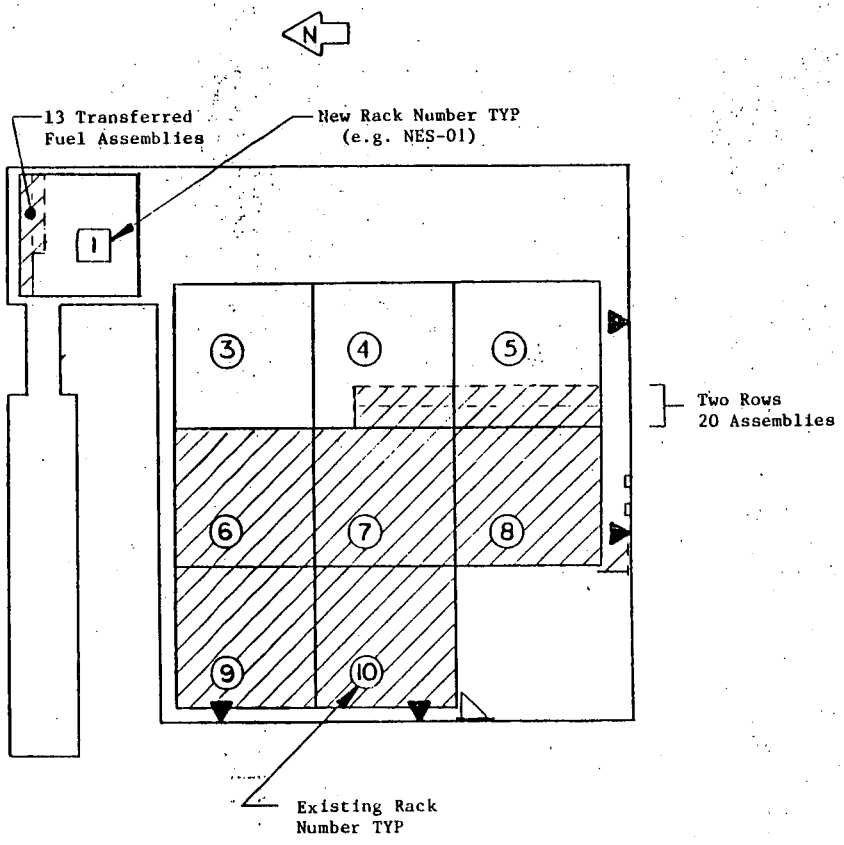

FIGURE 2
FUEL RACK INSTALLATION SEQUENCE

Installation of New Rack 1 and fuel transfer from existing racks 3 and 4.

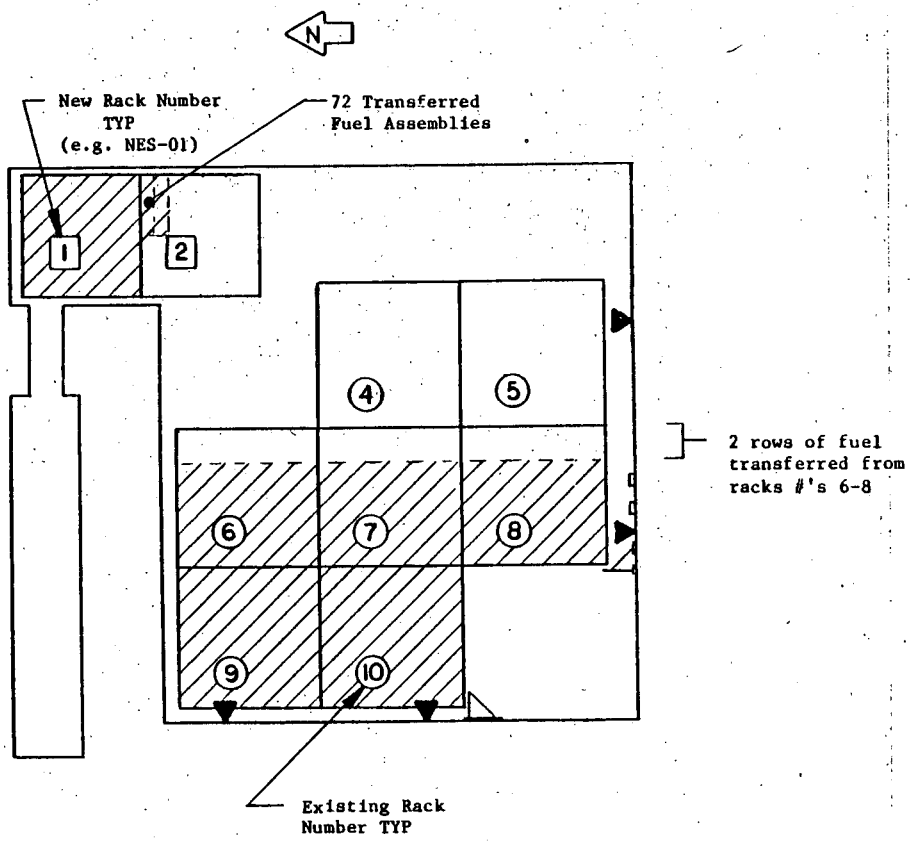

FIGURE 3
FUEL RACK INSTALLATION SEQUENCE

Installation of New Rack 2 and fuel transfer from existing racks 4 through 8.

NUCLEAR ENERGY SERVICES, INC.
DOCUMENT NO. 80A3501
PAGE _____ OF _____

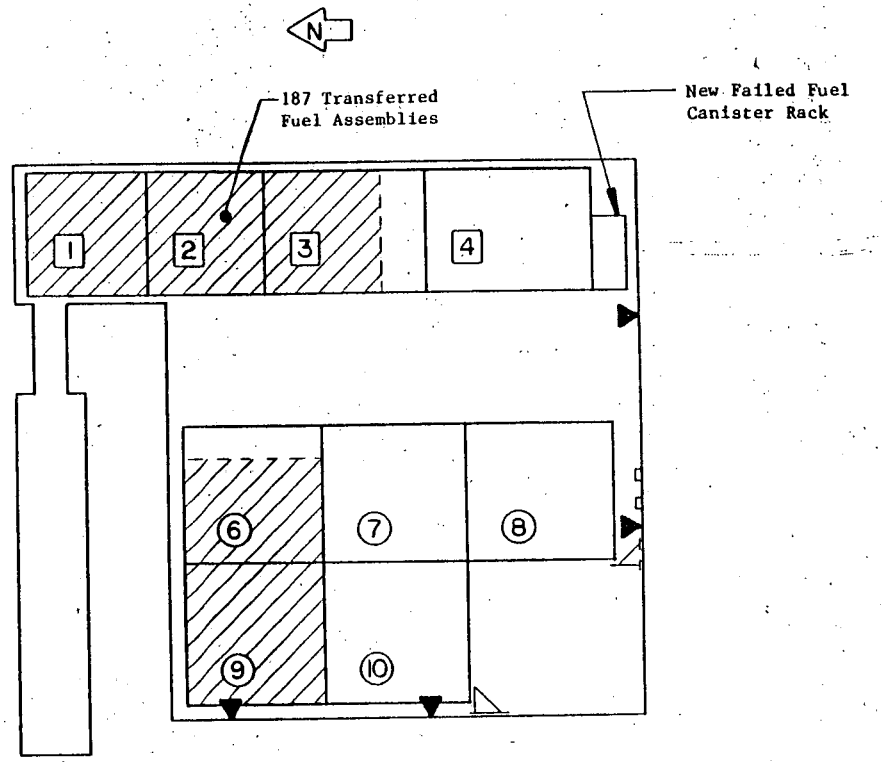

FIGURE 4
FUEL RACK INSTALLATION SEQUENCE

Installation of new racks 3 & 4 and fuel transfer from existing racks 7, 8, & 10

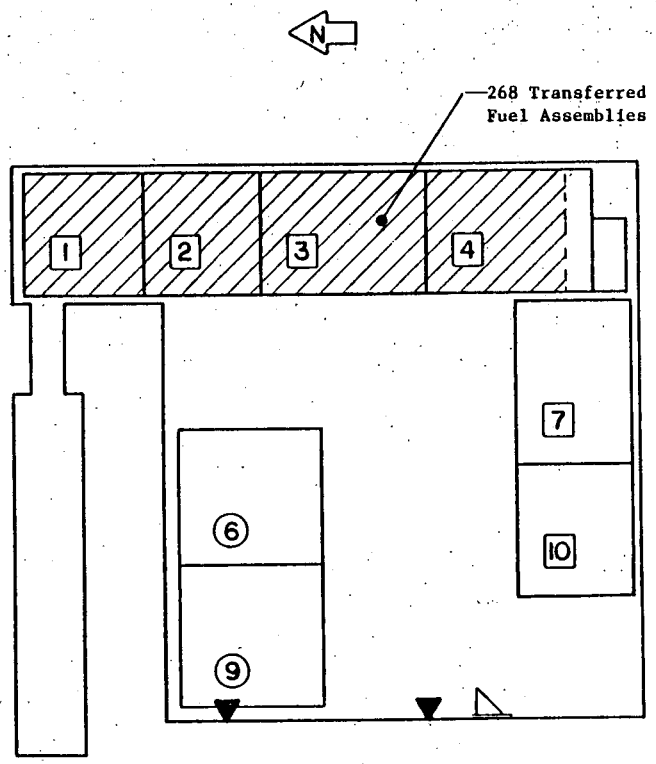

FIGURE 5
FUEL RACK INSTALLATION SEQUENCE

Installation of new racks 7 & 10 and fuel transfer from existing racks 6 and 9

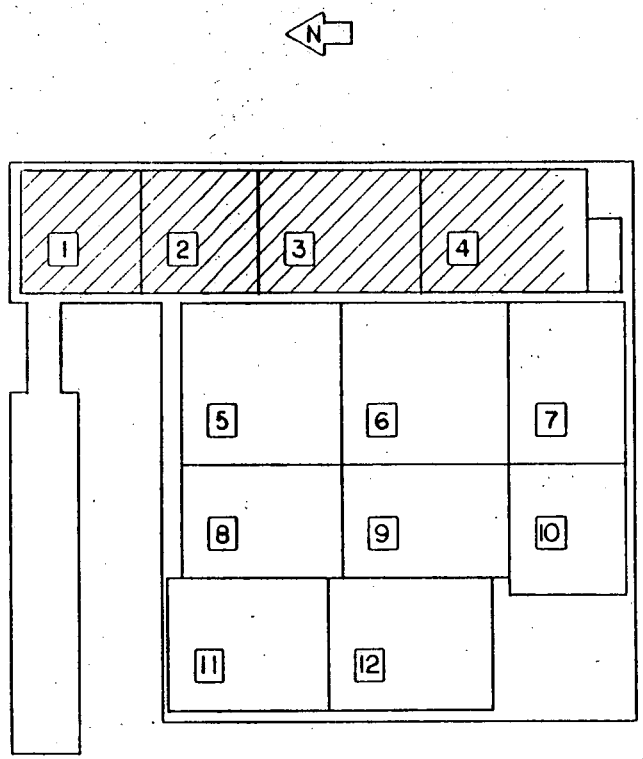

FIGURE 6
FUEL RACK INSTALLATION SEQUENCE

Installation of New Racks 11, 12, 6, 9, 5 & 8 in sequence

Response 7b. There is no equipment in the spent fuel storage building essential in the safe shutdown of the reactor or employed to mitigate the consequences of an accident which is beneath, adjacent to or otherwise within the area of influence of all loads that will be handled during the expansion modification.

Response 8: The expansion modification of the Indian Point Unit 2 Spent Fuel Pool will have designated travel paths to preclude the handling of any heavy load above spent fuel bundles. (The travel paths and sequence of removing and installing spent fuel stroage racks are shown in Response 7a above). This restriction on the motion of the spent fuel crane meets the intent of Section 5.1.6 of NUREG-0612 in that a failure of the load handling system will not exceed the guidelines of Section 5.1 of NUREG-0612.

Response 9: The specific loads and load combinations conform fully with 3.8.4-II-3 of the Standard Review Plan. The maximum uplift force is limited to the spent fuel bridge hoist with a lifting capacity of 2000 lbs. This maximum load will be controlled with a monitor control system with overload cutoff device which we are planning to install.

Response 10: The reference letter provides the change of number of fuel assemblies discharged for each cycle. The smaller number of fuel assemblies to be discharged (76 versus 90) allows additional cycles to fillup the available spaces. The revised schedule is provided in the following table:

Discharge Date	No. of Assy's	Sum of Assy's
6-76	72	72
1-78	60	132
6-79	68	200
1-81	72	272
6-82	59*	331
1-84	76	407
6-85	76	483
1-87	76	559
6-88	76	635
1-90	76	711
6-91	76	787
Full core discharge	193	980

Discussion of the results of the heat load was considered in the February 10, 1981 letter. More discussion shows in the following pages.

*Adjusted to maximize total pool heat generation

1. SUMMARY

Fuel storage racks have been designed to increase the present fuel storage capacity of the Indian Point 2 spent fuel storage pool to a total of 980 assemblies.

The maximum heat loads resulting from the expanded spent fuel storage have been calculated for both normal and abnormal fuel discharge cases (see Appendix A). Calculations indicate that the cooling capacity of the present fuel cooling system is adequate to handle the resulting normal and abnormal heat loads.

The increase of the pool water bulk temperature as a function of time has been determined assuming a failed heat removal system for normal and abnormal cases. (See Appendix B.)

The adequacy of natural circulation flow throughout the fuel racks to cool the fuel assemblies was verified (See Appendix C). Even with the bulk pool temperature at the maximum value of 155°F, sufficient circulation exists to preclude local boiling in any fuel assembly.

2. ASSUMPTIONS

2.1 MAXIMUM HEAT LOADS

The maximum heat loads, resulting from the expanded spent fuel storage capacity, have been calculated for two cases: the normal batch discharge and the abnormal full core discharge.

1. The assumed normal case consists of discharging a maximum of 76 fuel assemblies every 18 months with 90 hours of cooling time after shutdown. A plant capacity factor of 85% was assumed. The maximum heat load is scheduled to occur after the discharge of eleven batches with adequate storage kept in reserve for a full core discharge.

2. The assumed abnormal case is the discharge of a full core (193 assemblies) at any time during the cycle. The maximum heat load has been determined to occur soon after the startup following the scheduled refueling outage for the discharge of the eleventh batch. Cooling time to discharge is 400 hours after shutdown.

Decay heat generation is calculated according to Branch Technical Position APC SB 9-2, "Residual Decay Energy for Light Water Reactors for Long-Term Cooling", Dec. 24, 1975, including recommended uncertainty factors and actinide contributions. (For times greater than 10^7 seconds an uncertainty factor of 0.1 was used.) The reactor power used in the analysis is 2813 Mwt, which is 102% of rated power of 2758 Mwt.

2.2 HEAT-UP RATES

Maximum pool water bulk temperature is conservatively assumed to be 140° and 155°F respectively for normal and abnormal heat loads. The heatup rates and times to reach boiling temperature of 212°F are based on adequate mixing of the pool water.

2.3 VERIFICATION OF ASSEMBLY COOLING

The natural circulation flow is calculated by establishing a thermal-hydraulic balance for the worst row of assemblies (from a recent batch discharge with a 90-hour cooling period). The flow is maintained by the thermal driving head produced by the decay heat generation of each assembly. The pool is modeled as a large volume with a bulk temperature unaffected by local disturbances. The pressure losses considered in the analysis include:

1. Friction losses in the downcomer region, in the rack inlet plenum and in the fuel assembly.

2. Losses in turns.

3. Form losses in the fuel assemblies at the inlet, outlet, and grid locations.

Flow to the worst row of cells is assumed to be available from the narrowest downcomer only. Coolant from the cask handling area and rack-to-rack gaps is conservatively neglected. All fuel assemblies are assumed to have been freshly discharged (90-hour cooling time) with radial peaking factors of 1.2.

A maximum bulk pool temperature of 155°F is assumed.

3. RESULTS AND CONCLUSIONS

3.1 MAXIMUM HEAT LOADS

The maximum normal heat load anticipated would be encountered after the discharge of the eleventh batch into the pool. The pool would then contain 787 assemblies. Even if the remaining storage normally reserved for emergency full core discharge were to be used for additional normal batch discharges, after the eleventh batch, the incremental decay heat generation wil be minimal and certainly less than that calculated for the abnormal heat load. The calculated decay heat generation at that time is 18.6×10^6 Btu/hr, assuming a 90-hour cooling period after shutdown.

The maximum abnormal heat load anticipated would occur resulting from the emergency discharge of a full core (193 assemblies) into the pool two months after the discharge of the eleventh batch and one month after the subsequent startup. The pool would contain 980 assemblies. The calculated decay heat generation rate for this case is 24.5×10^6 Btu/hr, assuming a 400-hour cooling period. In addition, to demonstrate the lack of sensitivity of full core discharge timing the case of core off-load after 1.5 years of operation was also analyzed.

The Indian Point 2 spent fuel pool heat removal system is rated to remove 24.5×10^6 Btu/hr from the system with a pool water temperature of 155°F. Consequently, the cooling capacity is adequate for both the normal and abnormal discharge cases.

3.2 HEAT-UP RATES

In case of a complete failure of the Indian Point 2 spent fuel heat removal system, the maximum heat-up rates calculated for the maximum normal and abnormal heat loads anticipated are 8.9 and 11.7°F/hr, respectively. The total times available to perform repairs for the maximum normal and abnormal heat loads are 8.1 and 4.9 hours, respectively before makeup is required for pool boil-off. The makeup required is approximately 39 and 51 gpm of water for normal and abnormal heat loads.

3.3 VERIFICATION OF ASSEMBLY COOLING

The adequacy of the natural circulation flow to cool the worst row in the rack configuration was verified by establishing a thermal-hydraulic balance. The chief concern is the possibility of local boiling due to flow starvation in some cells of the rack matrix as a result of excessive pressure losses in the natural circulation loops established in the spent fuel pool.

The analysis shows that even under the most conservative assumption, the natural circulation in the pool is adequate to preclude boiling by a substantial margin, assuming a bulk pool temperature of 155°F. The maximum temperature increase in the assembly with minimum flow is 71.3°F, resulting in an outlet temperature of 226.3°F. This is below the saturation temperature of 239°F, corresponding to the static head at the top of the fuel assembly.

It should be noted that the maximum assembly outlet temperature of 226.3°F reported above is unlikely to occur in the pool, as it is the result of excessively conservative assumptions postulated to establish a calculational boundary. In the analysis, the major portion of the total pressure drop in the natural circulation loop is caused by the selection of the narrowest gap in the pool as the sole flow path to the bottom plenum from the water above the racks. The expected mode of natural circulation is for the coolant to reach the plenum via least-resistant flow paths, such as the cask area, the north wall downcomer gap of 11-9/10", the failed fuel elevator area, and between the 2-1/2" gap between racks, all of which have been neglected in the analysis.

APPENDIX A

INDIAN POINT 2 SPENT FUEL POOL

MAXIMUM HEAT LOADS

REF.

INDIAN POINT 2 SPENT FUEL POOL
MAXIMUM HEAT LOADS

1. STATEMENT OF PROBLEM

Calculate heat generation rates for NORMAL and ABNORMAL cases for fuel discharges scheduled.

2. ASSUMPTIONS

2.1 Core capacity is 193 assemblies 1

2.2 Maximum pool storage capacity is 980 assemblies. 2

2.3 Fuel discharge schedule assumed as follows *

DISCHARGE DATE	No. OF ASS'S	ΣNo of ASS'y
6-76	72	72
1-78	60	132
6-79	68	200
1-81	72	272
6-82	59	331
1-84	76	407
6-85	76	483
1-87	76	559
6-88	76	635
1-90	76	711
6-91	76	787
CORE DISCH	193	980

10

* Assuming 76 assemblies discharged every 18 months 1.

REF.

2.4 Normal cooling time is 90 hours after shutdown. For full core discharge, cooling time is 400 hours. 1

2.5 Batch exposures calculated assuming 85% capacity factor. The following is in the pool 90 hours after shutdown in June 1991. 1

BATCH #	DISCH DATE**	No. OF ASS'Y	EXPOSURE TIME *	COOLING TIME
1	6-76	72	1.5 YR	15 YR
2	1-78	60	3 YR	13.5 YR
3	6-79	68	4 YR	12 YR
4	1-81	72	4 YR	10.5 YR
5	6-82	59	4 YR	9 YR
6	1-84	76	4 YR	7.5 YR
7	6-85	76	4 YR	6 YR
8	1-87	76	4 YR	4.5 YR
9	6-88	76	4 YR	3 YR
10	1-90	76	4 YR	1.5 YR
11	6-91	76	4 YR	90 HR

* EXPOSURE TIMES HAVE BEEN APPROXIMATED TO NEAREST 1/2 YEAR. (EQUIVALENT FULL POWER OPERATING TIME).

** THESE DATES HAVE BEEN SELECTED FOR CALCULATIONAL PURPOSES ONLY.

2.6 Decay Heat Generation is calculated according to APCSB-9-2. The calculation includes recommended uncertainty factors and actinide contribution (for shutdown times $>10^7$ sec, k=0.1 was used). 3

2.7 Assume plant power of 2813 Mwt (9.6×10^9 Btu/hr) 1

REF.

3. HEAT LOAD CALCULATIONS

3.1 NORMAL Case

BATCH #	No. # Ass'y	EQUIV OP TIME	COOLING TIME	P/P₀ * (FULL CORE)	WEIGHTED P/P₀
1	72	1.5 YR	15 YR	5.39-5	2.01-5
2	60	3 YR	13.5 YR	6.99-5	2.17-5
3	68	4 YR	12 YR	8.18-5	2.88-5
4	72	4 YR	10.5 YR	8.48-5	3.16-5
5	59	4 YR	9 YR	8.80-5	2.69-5
6	76	4 YR	7.5 YR	9.15-5	3.60-5
7	76	4 YR	6 YR	9.62-5	3.79-5
8	76	4 YR	4.5 YR	1.05-4	4.13-5
9	76	4 YR	3 YR	1.30-4	5.11-5
10	76	4 YR	1.5 YR	2.27-4	8.93-5
11	76	4 YR	90 HR	3.94-3	1.55-3
	787				1.935-3

MAXIMUM HEAT LOAD (NORMAL CASE)

$$9.6 \times 10^{9} \times 1.935 \times 10^{-3} = 18.6 \times 10^{6} \text{ BTU/HR}$$

$$* \quad P/P_0 = (1+K)\left[P/P_0(\infty, t_s)\right] - P/P_0(\infty, t_0+t_s)$$

Uncertainty factor $K = 0.1$ used for $t_s > 10^7$ sec

10

11

REF.

3.2 ABNORMAL CASE

(A) Full Core Discharge in AUG 1991

This case assumes Batch #11 discharged during normal outage of 6-91 (see p. 2), plant started up in 7-91, full core discharged in 8-91. 400 hours later, the following would be in the pool:

BATCH #	NO. OF ASS'Y	EQUIV OP TIME	COOLING TIME	P/Po (FULL CORE)	WEIGHTED P/Po
1	72	1.5 YR	15 YR	5.39-5	2.01-5
2	60	3 YR	13.5 YR	6.99-5	2.17-5
3	68	4 YR	12 YR	8.18-5	2.88-5
4	72	4 YR	10.5 YR	8.48-5	3.16-5
5	59	4 YR	9 YR	8.80-5	2.69-5
6	76	4 YR	7.5 YR	9.15-5	3.60-5
7	76	4 YR	6 YR	9.62-5	3.79-5
8	76	4 YR	4.5 YR	1.05-4	4.13-5
9	76	4 YR	3 YR	1.30-4	5.11-5
10	76	4 YR	1.5 YR	2.27-4	8.93-5
11	76	4 YR	65 D	1.10-3	4.32-4
12A	64	30 DAYS	400 HR	1.02-3	3.38-4
12B	64	1.5 YR	400 HR	2.04-3	6.75-4
12C	65	3 YR	400 HR	2.14-3	7.19-4
	980				2.549-3

10

MAXIMUM LOAD (ABNORMAL CASE A)

$$9.6 \times 10^{9} \times 2.549 \times 10^{-3} = 24.5 \times 10^{6} \text{ BTU/HR}$$

REF.

(B) FULL Core Discharge in Jan 1993

This case assumes Batch #11 discharged during normal outage of 6-91, Plant startup up in 7-91, full core discharged 1½ years later, just prior to scheduled outage of 1-93.

BATCH #	NO OF ASS'Y	EQUIV OP TIME	COOLING TIME	P/P₀ (FULL CORE)	WEIGHTED P/P₀
1	72	1.5 YR	16.5 YR	5.20-5	1.94-5
2	60	3 YR	15 YR	6.74-5	2.09-5
3	68	4 YR	13.5 YR	7.89-5	2.78-5
4	72	4 YR	12 YR	8.12-5	3.03-5
5	59	4 YR	10.5 YR	8.48-5	2.59-5
6	76	4 YR	9 YR	8.80-5	3.47-5
7	76	4 YR	7.5 YR	9.15-5	3.60-5
8	76	4 YR	6 YR	9.62-5	3.79-5
9	76	4 YR	4.5 YR	1.05-4	4.13-5
10	76	4 YR	3 YR	1.30-4	5.11-5
11	76	4 YR	1.5 YR	2.27-4	8.93-5
12A	64	1.5 YR	400 HR	2.04-3	6.75-4
12B	64	3 YR	400 HR	2.14-3	7.09-4
12C	65	4 YR	400 HR	2.16-3	7.29-4
	980				2.53×10^{-3}

10

MAXIMUM HEAT LOAD (ABNORMAL CASE B)

$$9.6 \times 10^{9} \times 2.53 \times 10^{-3} = 24.3 \times 10^{6} \text{ BTU/HR}$$

APPENDIX B

INDIAN POINT 2 SPENT FUEL POOL

HEAT-UP RATES

REF.

INDIAN POINT 2 SPENT FUEL POOL MINIMUM HEAT-UP TIMES

1. STATEMENT OF PROBLEM

Determine the pool temperature as a function of time assuming a heat removal system failure.

2. ASSUMPTIONS

2.1 Maximum heat loads

Normal = 18.6×10^6 BTU/HR

Abnormal = 24.5×10^6 BTU/HR

2.2 Pool Geometry shown below

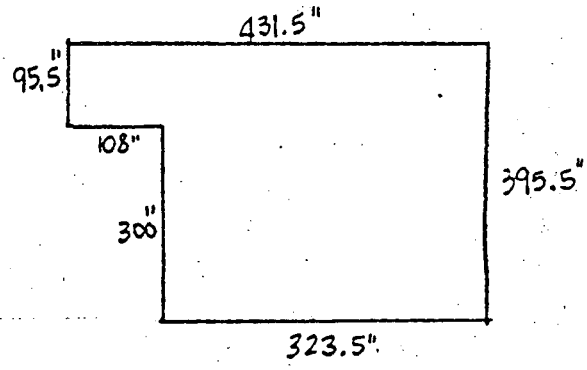

WATER LINE = 93'-8"

FLOOR ELEV = 54'-7¼"

WATER DEPTH = 468.75"

NES 105 (2/74)

REF.

2.3 UO_2 weight/assembly = 1155 lb 5
Zirc weight/assembly = 275 lb
Empty Rack weight (avg. est'd) = 23,000 lb

2.4 UO_2 density = 643 lb/ft^3
Zirc density = 406 lb/ft^3
Stainless density = 492 lb/ft^3
Water density @ 180°F = 60.6 lb/ft^3
Water C_p = 1.0 Btu/lb-°F

2.5 Pool full to capacity : 980 locations in 12 racks.

3. HEAT-UP CALCULATIONS

$$\text{Pool Vol} = \frac{1}{1728}\left[(95.5 \times 108) + (323.5 \times 395.5)\right] \times 468.75$$
$$= 37505 \text{ ft}^3 \checkmark$$

$$UO_2 \text{ volume} = \frac{1155 \times 980}{643} = 1760 \text{ ft}^3$$

$$\text{Zirc volume} = \frac{275 \times 980}{406} = 664 \text{ ft}^3 \checkmark$$

$$\text{Rack volume} = \frac{23{,}000 \times 12}{492} = 561 \text{ ft}^3$$

REF.

Net Water Vol = 37505 − 1760 − 664 − 561 = 34520 ft^3

Net Water Wt = 34520 × 60.6 = 2.092×10^6 lb

Max Normal Heat Load Heatup Rate.

$$\frac{18.6 \times 10^6}{2.092 \times 10^6} = 8.9 \ ^\circ F/hr$$

Max Abnormal Heat Load Heatup Rate

$$\frac{24.5 \times 10^6}{2.092 \times 10^6} = 11.7 \ ^\circ F/hr$$

→ Times needed to take preventive action
(from max bulk temp of 155 °F to boiling 212°F)

Normal = (212−140) / 8.9 = 8.1 HRS

Abnormal = (212−155) / 11.7 = 4.9 HRS

→ Evaporation Rate at 212 °F (h_{fg} = 970.3 Btu/lb)

Normal = $\frac{18.6 \times 10^6}{970.3}$ = 19169 lb/hr ≅ 39 gpm

Abnormal = $\frac{24.5 \times 10^6}{970.3}$ = 25250 lb/hr ≅ 51 gpm

APPENDIX C

INDIAN POINT 2 SPENT FUEL

VERIFICATION OF ADEQUATE COOLING

REF.

INDIAN POINT 2 SPENT FUEL POOL

VERIFICATION OF ADEQUATE COOLING

1. STATEMENT OF PROBLEM

Perform a thermal-hydraulic analysis to verify that the natural circulation in the expanded capacity rack configuration allows adequate cooling of all assemblies.

2. ASSUMPTIONS

Figure 2-1 shows the general arrangement of the Indian Point 2 storage pool. The row selected is considered the most critical area in terms of cooling for the assemblies.

2.1 The downcomer gap is 1.25" at the rack base. All other sources of cooling water (cask area, rack-to-rack spacings, other larger downcomer gaps) have been conservatively neglected.

2.2 All fuel assemblies in the 13-cell row have 4 years equivalent full power operation time, radial peaking factors of 1.2,

REF.

and have cooled 90 hours since shutdown. 1

2.3 The pool bulk water temperature is conservatively 155 °F.

2.4 The pool water depth is 39±1". The top of the rack is 185". Saturation temperature corresponding to the static head at the top of the rack is 239 °F.

2.5 Each bundle is isolated from adjacent assemblies by the cell walls and sits in its own thermal chimney. No credit for cross flows between assemblies at the inlet plenum level is taken.

2.6 Bundle Loss Coefficient K ($\Delta P/\frac{\rho V^2}{2g}$) is 24.1, including assembly entrance, exit and grid losses. This is based on the IP-2 core ΔP, corrected to account for fuel pin skin friction. 8

2.7 Water properties based on estimated bundle average of 170°F.

2.8 Bundle decay heat from APCSB 9-2, $P/P_0 = 3.94 \times 10^{-3}$ (T_0 = 4 years, T = 90 hours). Reactor rated power is 2813 Mwt. Core is 193 assemblies. 3

	REF.
2.9 The can is 9" square. Pitch is 10-15/16". Inlet channel height is 10" (between floor and bottom of rack beams).	2
2.10 The assemblies are 15x15, 204 fuel rods with 0.422" ØD, 21 guide thimbles, assumed occupied, with 0.545" ØD, 9 spacers.	5
2.11 Friction factors from Moody curves, CRANE, Flow of Fluids. Geometry factors from Idel'chik.	6 7
2.12 All rack dimensions from NES Drawings 80E3503, 80E3518 and 80E3521.	

REF.

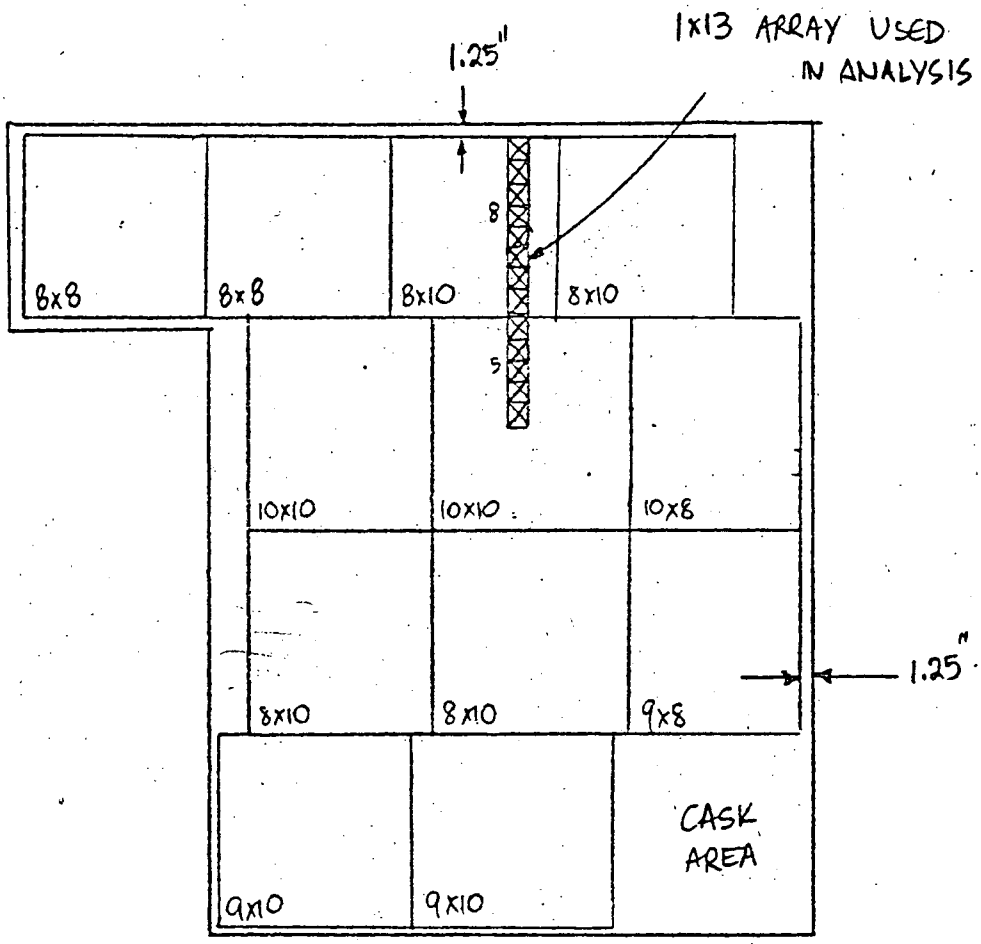

FIGURE 2-1 INDIAN POINT 2 FUEL STORAGE POOL AND RACK LAYOUT

REF.

3. ANALYSIS

3.1 DOWNCOMER LOSSES (ΔP_{DC})

$V = \frac{(GPM)}{(FA)(3600)}$

3.1.1 Wall Friction (ΔP_w)

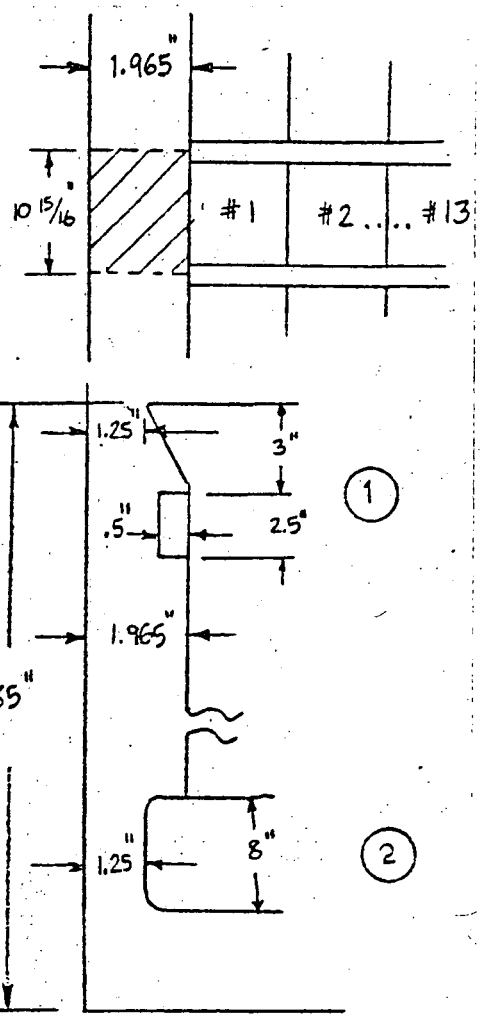

Flow Area, $A = 1.965 \times 10.94 = 21.50\ in^2$ ✓
$= 0.1493\ ft^2$

Wetted Perim, $P = 2 \times 10.94 = 21.88\ in$ ✓

Hyd Dia, $D_e = \frac{4A}{P} = \frac{4 \times 21.50}{21.88} = 3.93\ in$ ✓
$= 0.328\ ft$

Length, $L = 185"$ ✓

Water Properties @ 170°F

density $\rho = 60.8\ lb/ft^3$ ✓

visc $\mu = 0.83\ lb/hr\text{-}ft$

Assuming identical flow in each assembly:

Flow/assy (lb/hr)	Total Flow (lb/hr)	Velocity (ft/sec)	Re	f	$\Delta P_w = f \frac{L}{D_e} \frac{\rho V^2}{2g}$ (psi)
2500	32500	0.99	80800	0.0185	0.0056
5000	65000	1.99 ✓	161500 ✓	0.016 ✓	0.0196
7500	97500	2.98	242300	0.015	0.0411
10,000	130,000	3.98	323000	0.014	0.0684

REF.

3.1.2 Downcomer Restrictions (ΔP_r)

Flare opening and top bracing, Area ① modeled as indicated

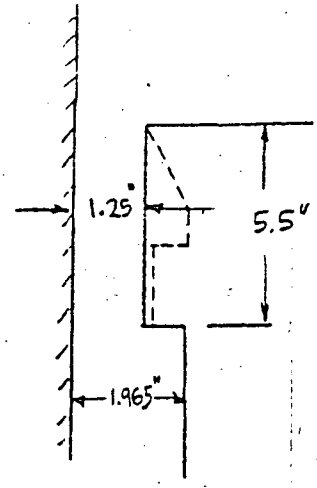

From Idel'chik (REF 7), DIAGRAM 3-18

$$k = \left(\xi_0 + \lambda \frac{L}{d_h}\right)\frac{1}{\bar{f}^2}$$

$\bar{f}$ = Area of orifice / Area of channel

$$= \frac{1.25 \times 10.94}{1.965 \times 10.94} = 0.636$$

$$d_h = \frac{4 \times \text{Orifice Area}}{\text{Orifice Perimeter}} = \frac{4 \times (1.25 \times 10.94)}{2 \times 10.94} = 2.5''$$

$$\frac{L}{d_h} = \frac{5.5}{2.5} = 2.2 \qquad \tau \propto \left(\frac{L}{D_h}\right) = 0.01$$

$$\xi_0 = 0.5 + (1-\bar{f})^2 + \tau(1-\bar{f})$$
$$= 0.5 + (1-0.636)^2 + 0.01(1-0.636) = 0.636$$

From Idel'chik, DIAG 2-2, Conduit with smooth walls for $Re = 10^5$, $\lambda = 0.018$

$$\therefore\ k = \left[0.636 + 0.018\,\frac{5.5}{2.5}\right]\frac{1}{(.636)^2} = 1.67$$

$$\Delta P_{r1} = K_1 \frac{\rho V^2}{2g}$$ where V is free channel (1.965").

REF.

Rack Base Area ② modeled as indicated

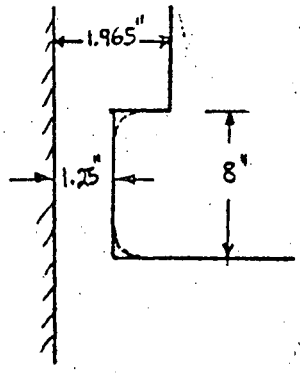

From Idel'chik, DIAG 11-29

$$k = \left(\xi_0 + \lambda \frac{l}{d_h}\right)\frac{1}{\bar{f}^2}$$

$\bar{f} = 0.636$ $\lambda = 0.18$

$d_h = 2.5''$

$l = 8''$

$\frac{l}{d_h} = \frac{8}{2.5} = 3.2$ ✓ $\tau = 0.0$

$$\xi_0 = 1 + 0.5(1-\bar{f}) + \tau\sqrt{1-\bar{f}}$$
$$= 1 + 0.5(1-0.636) = 1.182$$ ✓

$$k_2 = \left[1.182 + 0.018\frac{8}{2.5}\right]\frac{1}{(0.636)^2} = 3.065$$

$$\Delta P_{r_2} = k_2 \frac{\rho V^2}{2g}$$

(V in 1.965" channel)

TOTAL RESTRICTION $k = k_1 + k_2$

$= 1.67 + 3.065$

$= 4.735$ ✓

p6

Flow/Assy (lb/hr)	Total Flow (lb/hr)	Velocity (ft/sec)	ΔP_r (psi)
2500	32500	0.99	0.031 ✓
5000	65000	1.99	0.123
7500	97500	2.98	0.276
10,000	130,000	3.98	0.492

REF.

3.2 RACK BASE LOSSES (ΔP_B)

The rack base plenum losses are assumed to be negligible due to the unusual plenum height featured in the Indian Point 2 racks. The cell plates are about 18" above the pool floor, with approximately 10 inches between pool floor and bottom of rack base lattice. This provides a large volume of water that is available at all locations, especially since the whole pool floor area is open to all downcomers with no discrete channels.

Most of the cells receive coolant through 4.5-inch diameter rack base plate holes. The cells with feet are used in this analysis as they result in additional pressure drops.

3.2.1 Feet Support Holes (ΔP_{sh})

Two holes as indicated for each foot support configuration (NES Dwg 81E3518)

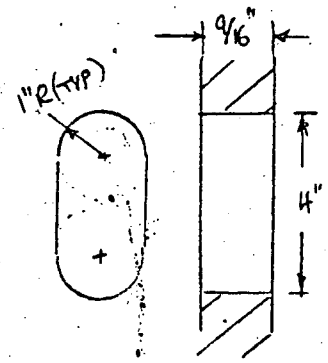

4

REF.

Flow Area, $A = 2\times2 + \frac{\pi}{4}2^2 = 7.142\ in^2$

Wetted Perim, $P = 2\pi + (2+2) = 10.283\ in$

Hyd Diam, $D_e = \frac{4A}{P} = \frac{4\times7.142}{10.283} = 2.78\ in$

From IDEL'CHIK, DIAG 4-18

$$k = \xi' + \lambda\frac{L}{D_h}$$

$$\frac{L}{D_h} = \frac{0.563}{2.78} = 0.20 \qquad \lambda = 0.018$$

p. 6

$$\xi' = 2.72$$

$$k = 2.72 + (0.018\times0.20) = 2.73$$

Flow/Ass'y lb/hr	Flow/HOLE lb/hr	Velocity (ft/sec)	ΔP_{SH} (psi)
2500	1250	0.115	0.0002
5000	2500	0.230	0.0009
7500	3750	0.345	0.0021
10,000	5000	0.461	0.0038

3.2.2 Base Plate Holes (ΔP_{ph})

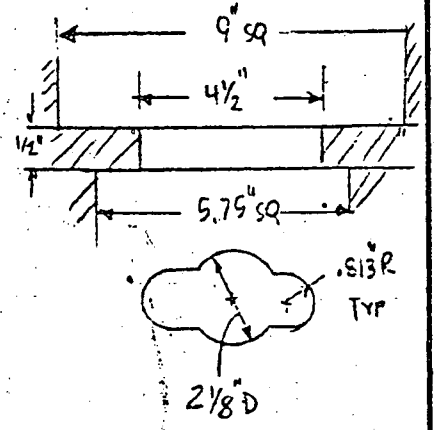

Flow Area, $A \cong \pi(0.813)^2 + \frac{\pi}{4}(2.125)^2 + (1.625)[4.5 - .813 - .813 - 2.125]$

$\cong 6.842\ in^2$

Wetted Perim, $P \cong 2\pi(0.813) + (\pi\ 2.125 - 2\times1.625) + 2[4.5 - .813 - .813 - 2.125] = 10.03\ in$

REF.

Hyd Diam, $D_c = \frac{4A}{P} = \frac{4 \times 6.842}{10.03} = 2.73$ in ✓

From IDEL'CHIK, DIAG 4-11

$$K = \xi_0 + \lambda \frac{l}{D_h}$$

$\lambda = 0.018$ ✓

$l = 0.5''$

$D_h = 2.73''$

$$\xi_0 = 0.5\left(1 - \frac{F_0}{F_1}\right) + \left(1 - \frac{F_0}{F_2}\right)^2 + \tau\left(1 - \frac{F_0}{F_1}\right)^{1/2}\left(1 - \frac{F_0}{F_2}\right)$$

$F_0 = A_{orifice} = 6.84 \text{ in}^2$

$F_1 = (5.75)^2 = 33.06 \text{ in}^2$

$F_2 = 9^2 = 81 \text{ in}^2$

$$\xi_0 = 0.5\left(1 - \frac{6.84}{33.06}\right) + \left(1 - \frac{6.84}{81}\right)^2 + 0.018\left(1 - \frac{6.84}{33.06}\right)^{1/2}\left(1 - \frac{6.84}{81}\right)$$

$$= .397 + .838 + .018(.890)(.916)$$

$$= 1.25 \checkmark$$

$$K = 1.25 + 0.018\,\frac{0.5}{2.73} = 1.25 \checkmark$$

Flow/assy (lb/hr)	Vel (ft/sec)	ΔP_{ph} (psi)	$\Delta P_8 = \Delta P_{sh} + \Delta P_{ph}$ (psi)
2500	0.24	0.0005	0.0007
5000	0.48	0.0019	0.0028
7500	0.72	0.0043	0.0064
10000	0.96	0.0076	0.0114

REF.

3.3 BUNDLE LOSSES (ΔP_b)

3.3.1 Bundle Friction (ΔP_{bf})

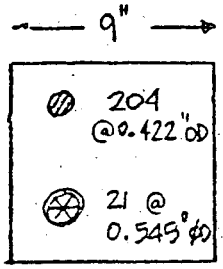

Rod Length = 150"

Flow Area, $A = 9^2 - 204\,\frac{\pi}{4}(.422)^2 - 21\,\frac{\pi}{4}(.545)^2$

$= 47.568\ in^2 = 0.330\ ft^2$ ✓

Wetted Perim, $P = 4 \times 9 + 204\,\pi(.422) + 21\,\pi(0.545) = 342.409$ in ✓

Hyd Diam, $D_e = \frac{4 \times 47.568}{342.409} = 0.556$ in ✓

Flow/Assy (lb/hr)	Vel ft/sec	Re	f*	ΔP_{bf} ✓
2500	0.035	403	0.298	0.0006
5000	0.069	806	0.149	0.0013
7500	0.104	1210	0.099	0.0019
10,000	0.138	1613	0.074	0.0025

$* f = \frac{120}{Re}$

9

3.3.2 Bundle Form Losses (ΔP_k)

K_{TOTAL} (based on rack cell area)

$= 24.1\,(.330/.266)^2 = 37.2$ ✓

Flow/Assy (lb/hr)	Vel (ft/sec)	ΔP_k (psi)	$\Delta P_b = \Delta P_{bf} + \Delta P_k$ (psi)
2500	0.035	0.0003 ✓	0.0009 ✓
5000	0.069	0.0012	0.0025
7500	0.104	0.0026	0.0045
10000	0.138	0.0046	0.0071

REF.

3.4 TOTAL PRESSURE LOSS

$$\Delta P_T = \text{Downcomer} + \text{Base} + \text{Bundle}$$
$$= \Delta P_{DC} + \Delta P_B + \Delta P_b$$

Flow/Assy (lb/hr)	ΔP_T (psi)
2500	0.047
5000	0.184
7500	0.407
10,000	0.720

REF.

5. NATURAL CIRCULATION HEAD

The driving force for the natural circulation flow is the density difference between the average hot column in the assemblies and the cooler bulk temperature in the downcomer.

The water column is assumed to be 15.5 ft (185"), conservatively neglecting any plume effects.

$$\Delta P = H(\rho_{COLD} - \rho_{HOT})$$

$$\rho_{COLD}\ (150°F) = 61.200\ lb/ft^3$$

$$\rho_{HOT}\ (200°F) = 60.096\ lb/ft^3$$

$$\Delta P_H = \frac{15.5}{50}(61.2 - 60.096)\frac{1}{144} = 0.00238\ psi/°F$$

$$\overline{\Delta T} = \overline{T}_{HOT} - 155°$$

Temp difference between hot column avg temp and downcomer

$$\overline{T}_{HOT} = \frac{155° + T_{OUT}}{2}$$

$$\therefore\ \overline{\Delta T} = \frac{155° + T_{OUT}}{2} - 155 = \frac{T_{OUT}}{2} - 77.5$$

$$\Delta P_H = 0.00238\left[\frac{T_{OUT}}{2} - 77.5\right]$$

Flow/ASSY lb/hr	T_{OUT} (p. 16)	ΔP_H
2500	249.1	0.1120
5000	202.0	0.0559
7500	186.4	0.0374
10,000	178.5	0.0280

REF.

4. BUNDLE HEAT GENERATION

Core Power = 2813 Mwt

= 9.6×10^9 Btu/hr

3.413 Btu/w-hr

Average Ass Power = $\frac{9.6 \times 10^9}{193} = 4.974 \times 10^7$ Btu/hr

$P/P_o = 3.94 \times 10^{-3}$ $T_o = 4$ yr

$T_s = 90$ hrs

Average Assy Power in Pool

$4.974 \times 10^7 \times 3.94 \times 10^{-3} = 195{,}979$ Btu/hr

Hot Assy Heat Generation in Pool

$195{,}979 \times 1.2 = 235{,}175$ Btu/hr

FLOW/ASSY	ΔT $T_{OUT} - T_{IN}$ (°F)	T_{OUT} $(155 + \Delta T)$ °F	$T_{BOILING}$ @ OUTLET °F
2500	94.1	249.1	239
5000	47.0	202.0	239
7500	31.4	186.4	239
10000	23.5	178.5	239

The combination of 155°F bulk temperature corresponding to the abnormal heat load case (400-hr cooling time), with the heat rate corresponding to a normally discharged assembly with 90-hr cooling is obviously conservative.

REF.

From FIG. 1

THE minimum flow per assembly = 3300 lb/hr

$$\Delta T_{max} = \frac{235,175 \text{ Btu/hr}}{3300 \text{ lb/hr}} \frac{\text{lb °F}}{\text{Btu}} = 71.3 \text{ °F}$$

$$T_{OUTLET,MAX} = 155 + 71.3 = 226.3 \text{ °F}$$

$$< T_{sat} = 239 \text{ °F}$$

The maximum assembly outlet temperature is, therefore, substantially less than the boiling temperature of 239 °F. It should be noted that even this value of 226.3 °F, is unlikely to occur in the pool, since a major portion of the total pressure drop calculated is caused by the 1.25" downcomer gap, conservatively assumed to provide the only path to the plenum from the pool bulk water above the racks. The anticipated mode of natural circulation is for the coolant to reach the plenum via least-resistance flow paths, such as the cask area, the north wall downcomer gap of 11-9/16" and between the 2.5"-gap between racks.

REF.

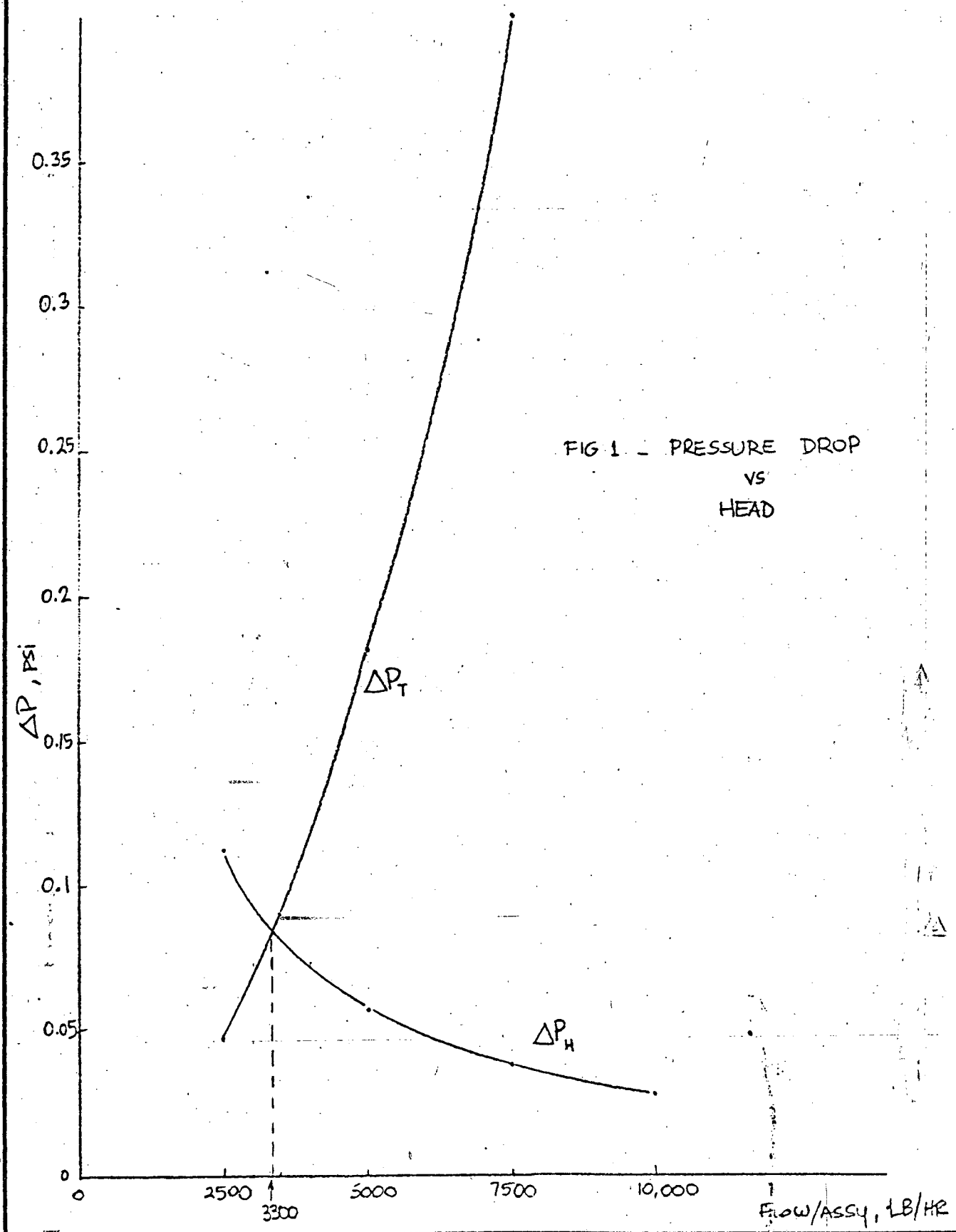

FIG 1 - PRESSURE DROP VS HEAD

REF.

REFERENCES FOR APPENDICES A, B, C

1. CON ED SPEC MP79-001, Section 6.5.1
2. NES QAPP 81A0606, APP A
3. Branch Technical Position 9-2, Residual Decay Energy for Light Water Reactors for Long-Term Cooling, 11-24-75.
4. NES Drwg 81E3521
5. CON ED SPEC MP79-001, TABLE 1
6. CRANE, Flow of Fluids, Tech. Paper 410, A-24.
7. Idel'chik, Handbook of Hydraulic Resistance, AEC-tr-6630.
8. Telecon between A. Uziel (NES) and D. Speyer (Con Ed), 12-6-79
9. Rohsenow & Hartnett, Handbook of Heat Transfer, p. 7-129
10. Telecopy to A. Uziel (NES) from Con Ed, 12-2-80.
11. NRC letter, O.D. Parr to J.C. Saldarini, Ebasco Services Inc, 9-26-80

Response 11: The heat removal capability Q, of the spent fuel pool heat exchanger was obtained, as a function of pool temperature, using the following shell side (i.e., component cooling fluid) energy balance, tube side (pool water) energy balance, and the equation of heat transfer,

$Q = WC\ (T_{out} - T_{in})$

$Q = wc_p\ (t_{out} - t_{in})$

$Q = UA\,\Delta T_m$

where,

W = shell-side mass flow rate = 1.1×10^6 lb/hr

w = tube-side mass flow rate = 1.1×10^6 lb/hr

C = shell-side fluid specific heat = 1.0 Btu/lb - ^oF

c_p = tube-side fluid specific heat = 1.0 Btu/lb - ^oF

U = overall heat transfer coefficient = 310 Btu/hr -^oF -ft^2

A = total heat transfer area = 2000 ft^2

ΔT_m = The mean temperature difference as derived for a one shell pass, two tube pass configuration (mixed cocurrent/countercurrent flow), is used, and:

The removal capability versus pool temperature was determined - see Figure 1. The FSAR results are compared to this calculation, for a pool temperature of 120^oF (i.e., t_{out}).

	t_{in} (°F)	T_{out} (°F)	Q (Btu/hr)
Present calc.	109.99	101.31	11.01×10^5
IP2 FSAR	109.9	101.5	11.15×10^5

The heat load in the pool (for the abnormal case) versus time, and pool water temperature versus time, are shown in Figure 2 (for reference, Figure 3 shows the normal case).

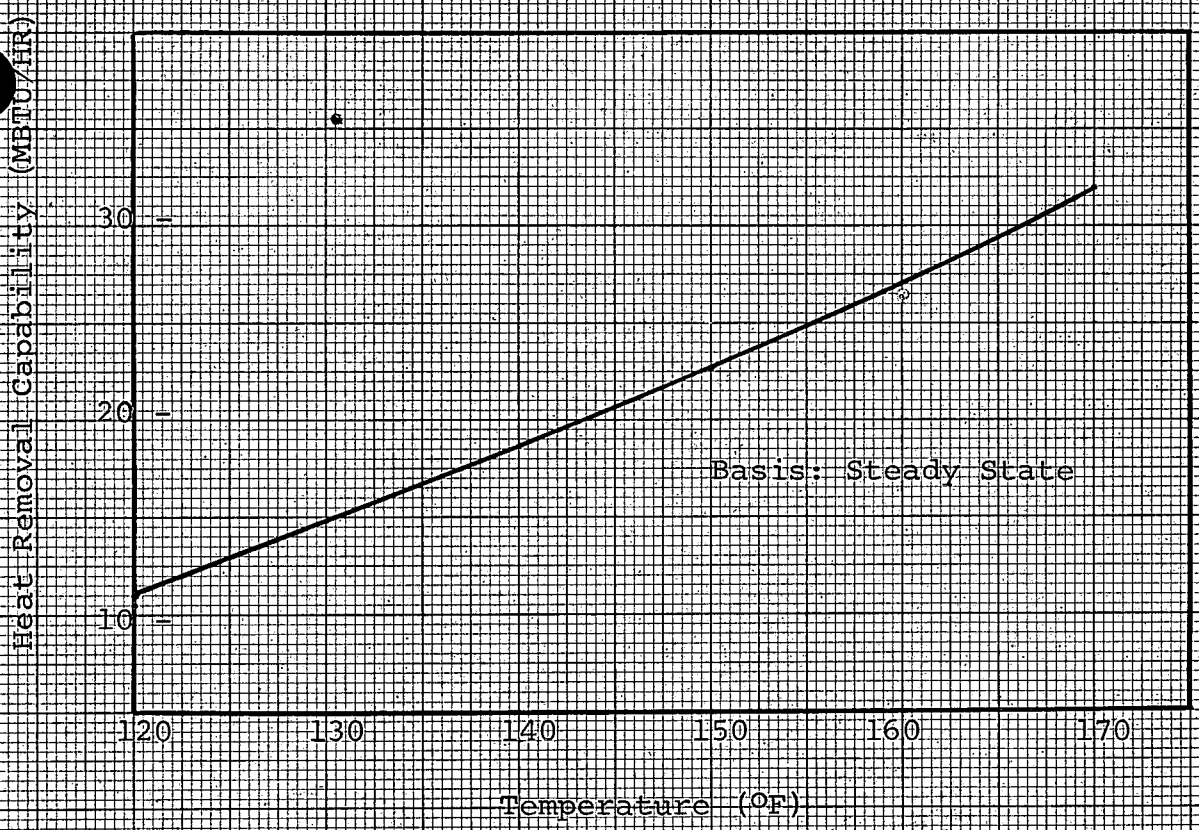

Figure 1. Heat Exchanger Capability vs. Pool Temperature

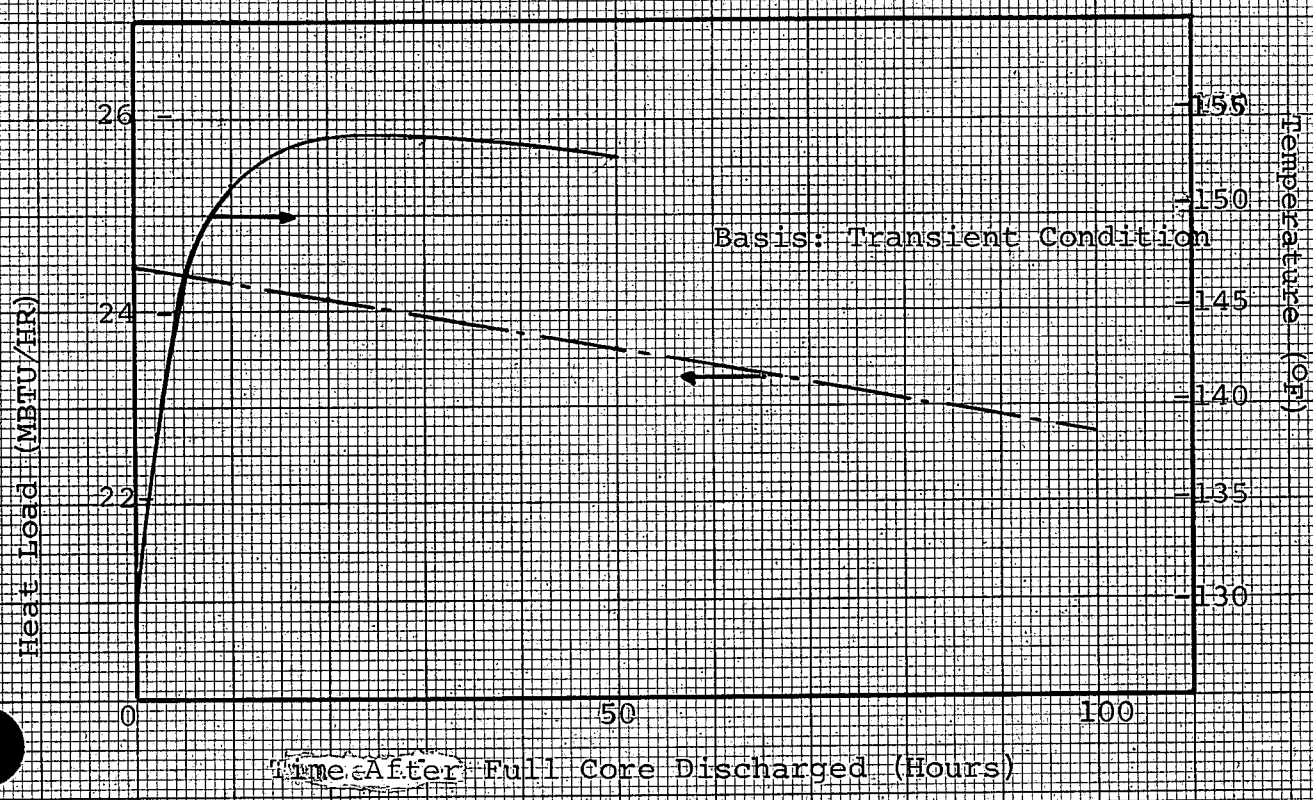

Figure 2. Decay Heat Load and Pool Temperature vs. Time for the Abnormal Full Core Discharge Case

NO. 318 20 DIVISIONS PER INCH BOTH WAYS. 150 BY 200 DIVISIONS.
Codex GRAPH PAPER IN STOCK DIRECT FROM CODEX BOOK CO., NORWOOD, MASS. 02062
PRINTED IN U.S.A.

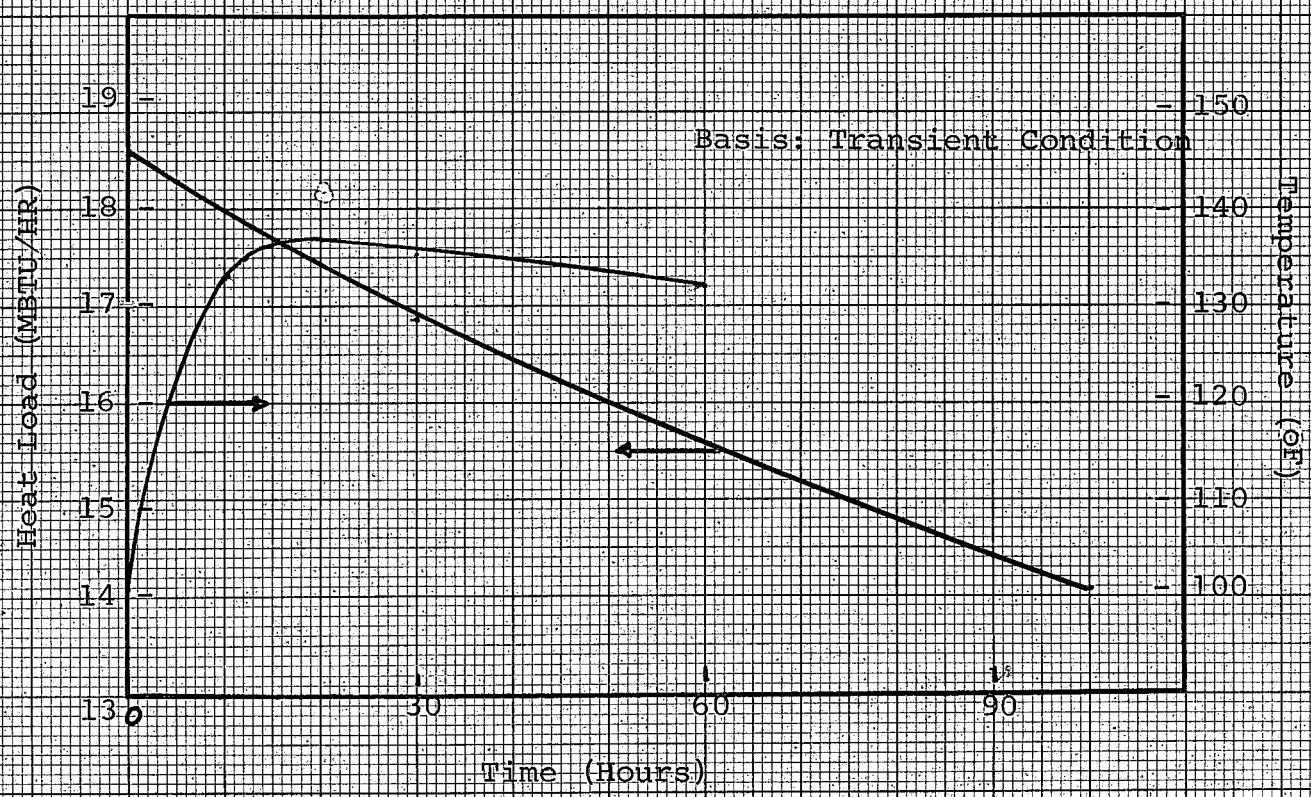

Figure 3 Decay Heat Load and Pool Temperature vs Time after Last Batch Is Discharged for the Normal Batch Discharge Case

NO. 318 20 DIVISIONS PER INCH BOTH WAYS, 150 BY 200 DIVISIONS. codex® GRAPH PAPER IN STOCK DIRECT FROM CODEX BOOK CO., NORWOOD, MASS. 02062 PRINTED IN U.S.A.

Additional clarifications are as follows:

(1) The minimum rack-to-wall distance has been established at 1¼" at the rack top flare level to accommodate sliding and lateral deflection of the cells. Under nominal conditions, the same gap will exist at the rack base level for sliding only, except that the gap maybe reduced to a minimum of 3/4" if necessary during installation to accommodate rack fabrication tolerance and wall out-of-plumbness. It should be noted that the gap along most of the height of the rack is actually 1.965" (see attachment 1). Since the Thermal-Hydraulic Report (NES 81A0609) postulated excessively conservative assumptions to establish a calculational boundary-while simultaneously ignoring less-resistant flow paths in the large wall-to-rack and rack-to-rack gaps, cask area and failed fuel rack area no technical justification exists to incorporate a local reduction to the rack base gap at non-nominal conditions into the calculations. In fact as shown in (2), below, floor pressure drop is negligible - thus coolant is free to distribute itself to assemblies via all downcomer flow areas.

(2) The 90° turn losses from the ten-inch high bottom plenum into the rack storage cells were calculated to be negligible (0.0006 psi) in comparison with total calculated pressure drop (0.08psi). This is due to the relatively spacious plenum in the IP-2 racks with the corresponding low plenum velocities. The floor friction losses similarly result in a negligible pressure drop (0.0001 psi).

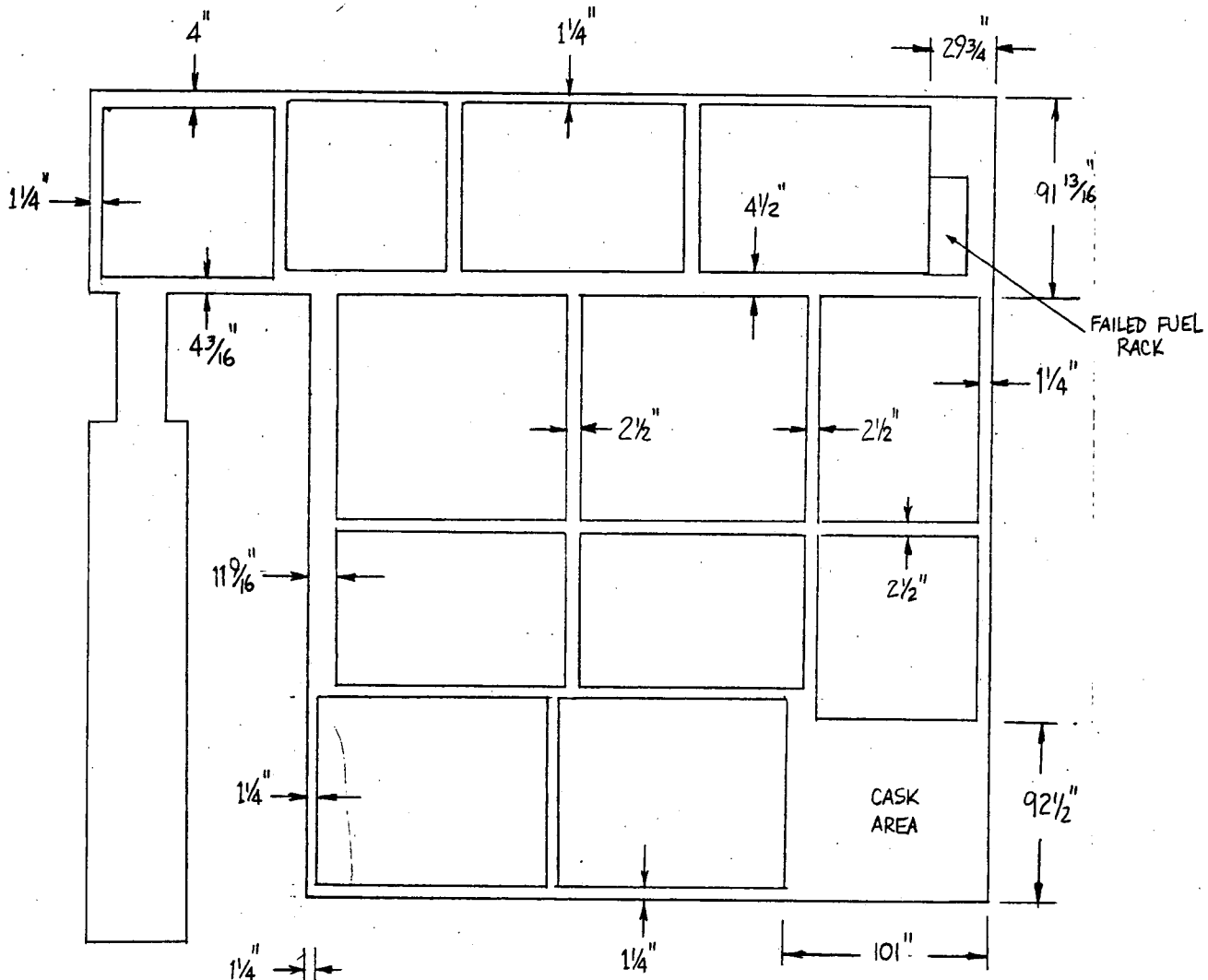

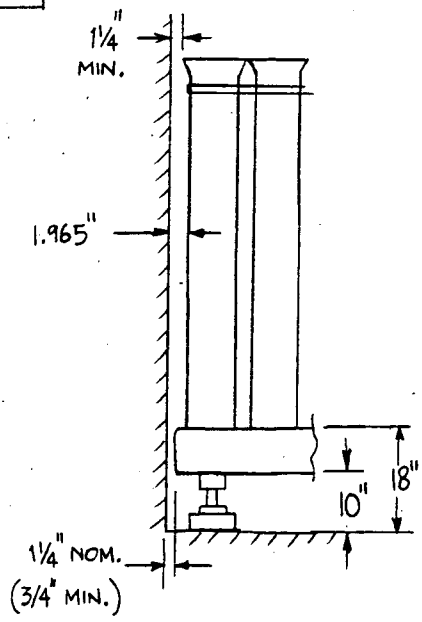

ATTACHMENT 1
RACK LAYOUT IN IP-2 POOL

(3) A thermal power 2813 MWt (102% of rated power of 2758 MWt) was used in the Report (See Response 10).

(4) A recalculation of maximum temperature increase in an assembly using the average assembly heat generation results in 65°F corresponding to 3000 lb/hr minimum flow/assembly. This is lower than the 71.3°F reported previously which obviously remains as more conservative.

(5) The radial peaking factor of 1.2 used in the T/H Report is very conservative based on the following analysis:

a. Under the normal condition most assemblies will reside in core for three (3) cycles. A calculation shows that the maximum average assembly peaking factor is 1.035. (Fig. 3.2.1-3, Indian Point 2 FSAR for general reference).

b. Under the abnormal condition (to discharge a full core), a particular assembly may have a value of above 1.2, (Fig. 3.2.1-2) Indian Point 2 FSAR for general reference). However, the decay heat for the hottest assembly is considerably lower than that in the normal condition (Ref. T/H Report, 81A0609) and the calculation of the outlet temperature in the abnormal case utilized the normal case decay heat.

Therefore, the 1.2 radial peaking factor used is conservative in both cases.

(6) The possibility of the wall-to-rack gap reduction as a result of rack sliding during a seismic event has been considered in the thermal-hydraulic evaluation. Calculations

show that even if the wall-to-rack gap on one whole side of the pool were to disappear due to intimate contact between rack base and adjacent wall, the relatively large rack bottom plenum (10") would generate a negligible ΔP across the floor (0.0001 psi) even if the total flow were assumed to become available from the opposite end of the pool (which would have a larger gap than its nominal value). Of course, the overall average downcomer gap would remain a constant regardless of actual rack layout in the pool.

(7) From countercurrent flooding correlations it can be shown that countercurrent flow is readily established in a cell with a fuel assembly that experiences a flow blockage at its bottom entry hole.

Using a Wallis flooding correlation (G.B. Wallis, <u>One-dimensional Two-phase Flow,</u> McGraw Hill, 1969) a value of j_g^* (the dimensionless volumetric gas flux) of 0.09 was calculated. This is substantially lower than the 0.7-1.0 range, normally accepted as the limiting values. Consequently, if total flow blockage to the bottom of an assembly were to occur, adequate cooling would be maintained by pool water draining into the rack cell (fuel assembly) and replace the mass inventory displaced due to evaporation as exiting vapor.

Response 12: Three principal methods are available for providing makeup water to the Spent Fuel Pit.

1. Demineralized water (unborated) from the Primary Water Tank.
2. Borated water from the Refueling Water Storage Tank.
3. Non-demineralized water from the fire protection system.

Source 1 is supplied from a 165,000 gallon primary water tank by two 150 gpm primary water makeup pumps. The primary water storage tank and the makeup pumps are seismic Class 1. Piping involved is listed below:

Line	Spec. Class	Seismic Class*	Quality Group**
184	3,4-PW-151N	I	B
33	1½,3-PW-151N	I & II	C
103	2-PW-151N 2-PW-151R	I & II	C
328	8-AC-151R	II	C

The following four(4) pages discuss the Loading Combination and Stress Limits for OBE and SSE Loadings:

*Seismic Class - defined in IP-2 FSAR Appendix A, Design Criteria For Structures and Equipment

**Quality Group - define in NRC Reg. Guide 1.26 (Rev. 3) Quality Group Classifications and Standard Line Spec.

LOADING COMBINATIONS AND STRESS LIMITS FOR OBE AND SSE LOADINGS

A. FSAR LOADING COMBINATION NO. 2*

Normal and Design Earthquake Loads (OBE; Horizontal Ground Acc. = 0.1 g)

$P_L + P_B - 1.2\ S$

$P_L = .5\ S$ (Long Press Stress)

$P_B = P_{DW} + P_S$

$P_{DW} = .1\ S$

$P_S = .2\ S$

$P_{DW} + P_S + P_L = .1\ S + .2\ S + .5 = .8\ S$

Allowable $= 1.2\ S$

Leftover $= .4\ S$

B. FSAR LOADING COMBINATION NO. 3*

Normal and Maximum Potential Earthquake Loads (SSE) Horizontal Ground Acc. = .15 g)

$P_L + P_B - 1.2\ (1.5)\ S$

$P_L = .5\ S$

$P_{DW} = .1\ S$

$P_S = \frac{.15}{.10} \times .2 = .3\ S$

$P_{DW} + P_S + P_L = .1\ S + .3\ S + .5\ S = .9\ S$

---

*FSAR Appendix A, Table A.3-1. (Attachment I)

Allowable =1.8 S

Left over = .9 S

C. Comparison of A & B above indicates that for Class I piping for Indian Point 2, OBE load combination.

D. Class 2 Piping for IP2 is designed for OBE loads (0.1 g horz. ground acc.) - See FSAR Appendix A Page A-3 (attach). As OBE controls the design of Class I piping, reevaluation of IP2 Class 2 piping is not required.

FROM IPZ APPENDIX A FSAR

TABLE A.3-1 - LOADING COMBINATIONS AND STRESS LIMITS

LOADING COMBINATIONS	VESSELS	PIPING	SUPPORTS
1. Normal Loads	$P_m \leq S_m$ $P_L + P_B \leq 1.5\ S_m$	$P_m \leq S$ $P_L + P_B \leq S$	Working Stresses or Applicable Factored Load Design Values
2 Normal + Design Earthquake Loads	$P_m \leq S_m$ $P_L + P_B \leq 1.5\ S_m$	$P_m \leq 1.2\ S$ $P_L + P_B \leq 1.2\ S$	1-1/3 Working Stresses or Applicable Factored Load Design Values
3. Normal + Maximum Potential Earthquake Loads	$P_m \leq 1.2\ S_m$ $P_L + P_B \leq 1.2\ (1.5\ S_m)$	$P_m \leq 1.2\ S$ $P_L + P_B \leq 1.2\ (1.5\ S)$	Deflections and Stresses of Supports Limited to Maintain Supported Equipment Within their Stress Limits
4. Normal + Pipe Rupture Loads	$P_m \leq 1.2\ S_m$ $P_L + P_B \leq 1.2\ (1.5\ S_m)$	$P_m \leq 1.2\ S$ $P_L + P_B \leq 1.2\ (1.5\ S)$	Deflections and Stresses of Supports Limited to Maintain Supported Equipment Within Their Stress Limits

Where P_m = primary general membrane stress; or stress intensity

P_L = primary local membrane stress; or stress intensity

P_B = primary bending stress; or stress intensity

S_m = stress intensity value from ASME B & PV Code, Section III

S = allowable stress from USAS B31.1 Code for Pressure Piping

All components, systems and structures classified as Class I are designed in accordance with the following criteria:

1. Primary steady state stresses, when combined with the seismic stress resulting from the response to a ground acceleration of 0.05g acting in the vertical and 0.1g acting in the horizontal planes simultaneously, are maintained within the allowable stress limits accepted as good practice and, where applicable set forth in the appropriate design standards, e.g., ASME Boiler and Pressure Vessel Code, USAS B31.1 Code for Pressure Piping, ACI 318 Building Code Requirements for Reinforced Concrete, and AISC Specifications for the Design and Erection of Structural Steel for Buildings.

2. Primary steady state stresses when combined with the seismic stress resulting from the response to a ground acceleration of 0.10g acting in the vertical and 0.15g acting in the horizontal planes simultaneously, are limited so that the function of the component, system or structure shall not be impaired as to prevent a safe and orderly shutdown of the plant.

All Class II structures and components are designed on the basis of a static analysis for a ground acceleration of 0.05g acting in the vertical and 0.1g acting in the horizontal directions simultaneously.

The structural design of all Class II structures meets the requirements of the applicable building code which is the "State Building Construction Code" State of New York, 1961. This code does not reference the Uniform Building Code.

Table A.1-1 gives the damping factors used in the design of components and structures.

Source 2 is supplied from the 350,000 gallon Refueling Water Storage Tank by the 100 gpm Refueling Water Purification Pump. The Refueling Water Storage Tank is seismic class I while the Refueling Water Purification Pump is seismic class II. Piping involved is listed below:

Line	Spec. Class	Seismic Class	Quality Group
155	16SI151R	I	B
183	2-AC-151R 2-SI-151R	I & III	B,C
135	1&2-AC-151R	III	C
126	2,3-AC-151R	III	C
127	3-AC-151R	II & III	C
328	8-AC-151R	II	C

Source 3 is supplied via hose connections for the Plant Fire Protection System. This water source is described in Revision 1 to "Review of the Indian Point Station Fire Protection Program," submitted to the NRC by letter dated April 15, 1977, and also in the Fire Protection Safety Evaluation Report issued by the NRC Regulatory Staff in conjunction with Amendment No. 46 to DPR-26 on January 31, 1979.

Each of the above three makeup water sources can be activated in a relatively short period, well within the 4.1 hour require-ment.

Reference Drawings Attached

1. Con Edison Drawing No. A200764: Flow Diagram, Chemical and Volume Control System, Sheet No. 1
2. Ibid Drawing No. A 200720, Sheet No. 2
3. Con Edison Drawing No. A200777: Flow Diagram, Primary Makeup Water System Nuclear Steam Supply Plant

4. Con Edison Drawing No. A200719: Flow Diagram, Auxiliary Safety Injection System.

5. Con Edison Drawing No. A200715; Flow Diagram, Auxiliary Coolant System.

6. Con Edison drawing No. A201030: Yard Fire Protection Piping, Plan and Diagram of Plant Fire Protection System.

Response 13: The maximum potential kinetic energy capable of being developed by any object normally handled above stored spent fuel if dropped, is well within the boundary of a cask drop analysis. The radiological evaluation of a cask drop was performed and reported in NES 81A0614. Results indicate that the off-site doses to the total body and thyroid in a cask drop accident are well below the limit specified in 10 CFR Part 100. At present, the cask is not used at Indian Point Unit No. 2. The objects normally handled over or near spent fuel, which are greater than 200 lbs, are: the thimble plug handling tool, the burnable poison handling tool, the proposed new RCC changing tool, the spent fuel handling tool, the inspection stand and a new fuel assembly and its associated handling tool. All of these have kinetic energies below that developed by a cask drop.

Response 14: Based on the information provided in our letter, specifically, the reduced power and a modified discharge schedule, the maximum heat load for normal (see Table in Response 10) and full core discharge (full core discharged at 400 hours after reactor is shutdown) cases are calculated to be 18.5x106Btu/hr and 24.5x106 Btu/hr, respectively. These heat loads would cause boiling of the pool water in 8.1 hours and 4.9 hours, for normal and full-core cases, respectively, if the heat removal system completely fails. This is based on an initial pool temperature corresponding to the respective maximum heat load (Figure 1 of Response 11) at a steady state condition. To delay these boiling times to ten hours would require that the maxium heat load be reduced to 16.3x106 BTU/hr. Based on the figure in next page, the decay time before off load needed to delay boiling for ten hours is 6 days for the normal case and 48 days for the full core case.

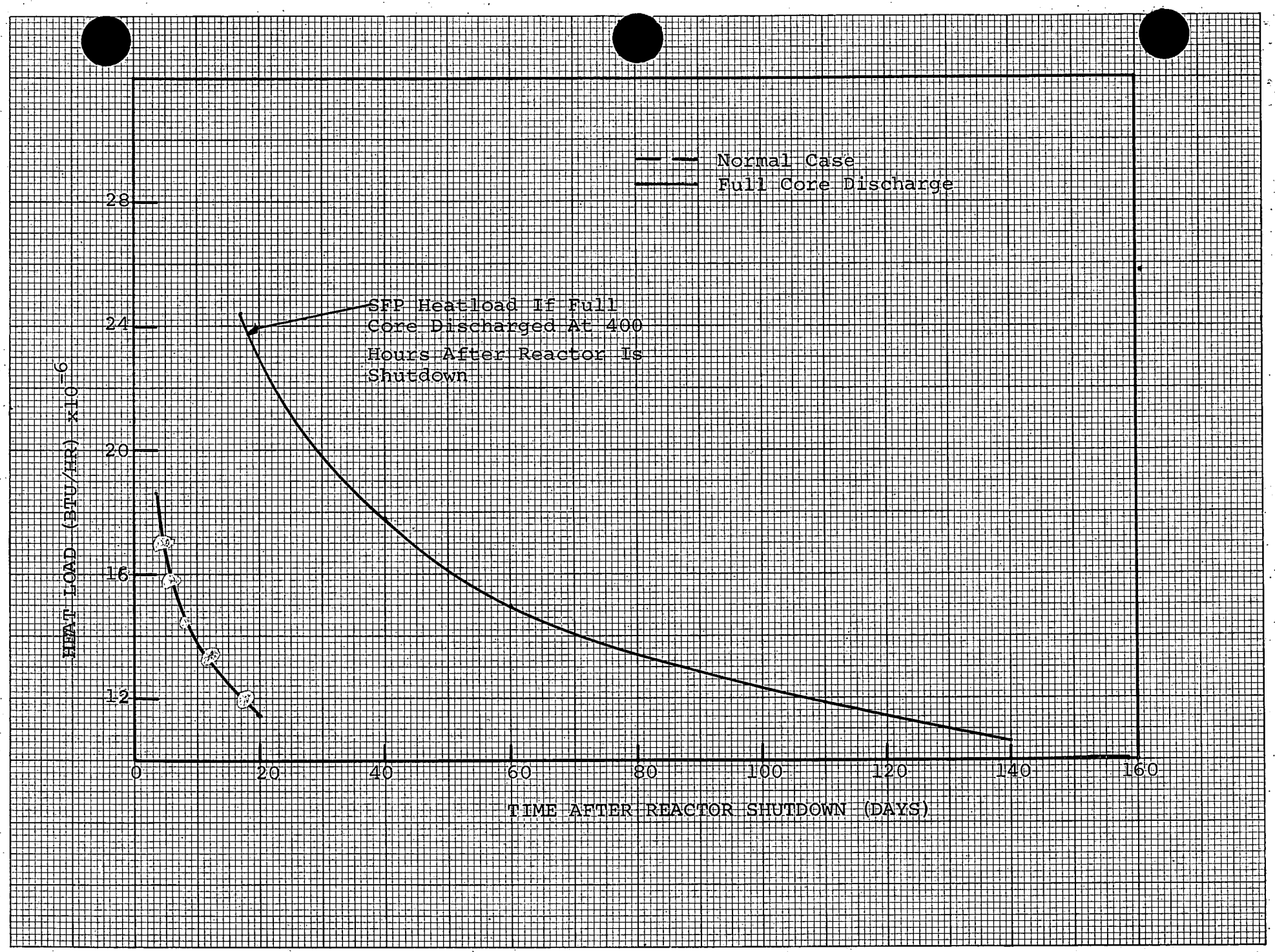

NO. 318 20 DIVISIONS PER INCH BOTH WAYS. 150 BY 200 DIVISIONS.
CODEX GRAPH PAPER IN STOCK DIRECT FROM CODEX BOOK CO., NORWOOD, MASS. 02062
PRINTED IN U.S.A.

Response 15: The high density spent fuel storage modification will require no change to the spent fuel pit cooling loop (SFPCL). The modification will have insignificant impact on the level of pool water purity with respect to visual clarity and activated corrosion and fission product buildup which are principally a function of the last discharged fuel (i.e. highest activity). Although it was assumed that the number of defective fuel assemblies increases in proportion to the increased spent fuel storage capacity, the original basis and the present basis are unchanged (i.e. one third of a core discharged in each cycle during normal operation and a full core discharged during abnormal conditions). Thus, no modification to the SFPCL is required.

Response 16: Water samples are drawn at approximately weekly intervals from the spent fuel pool and analyzed to determine pool water chemistry. The limiting values are:

Chloride: less than 0.15 ppm

Fluoride: less then 0.15 ppm

Boron: Pool is borated to match that required in the reactor coolant system during refueling operation. pH expected range 4.5 to 5.5 (Function of Boron Concentration).

Demineralizer resin is replaced when the decontamination factor falls below a value of 5 by measuring the specific activity of Co-58, Cs-134, or Cs-137. These limits are based on the recommendations set forth in Westinghouse document SIP-5.

Response 17: The following is a list of attached NES drawings that will provide the required information:

80E3503 - Fuel Storage Rack Arrays

80E3509 - 10x10 Base Structure Type 1

80E3517 - Base Structure Sections

80E3521 - Fuel Storage Rack Arrangement In Pool Sh. 1 of 2

80E3522 - Fuel Storage Rack Arrangement In Pool Sh. 2 of 2

Response 18: Attached Westinghouse Drawings are:

1548E49 - IPP HIPAR & LOPAR 15x15 Spent Fuel Assy Handling Tool

1547E55 - Indian Point No. 2 Fuel Assy Outline and Reprocessing

Response 19: The spent fuel assembly is handled with a grapple tool attached to the one-ton capacity hoist of the fuel handling bridge. The upper limit control switch on the hoist will stop the lift when the spent fuel assembly is approximately 13 inches above the new storage racks, or 25 inches above the existing storage racks.

Response 20: Mechanical stops located on the crane rails prevent travel of the crane over the spent fuel pit. Removal of these stops is controlled by the Fuel Storage Building Crane Operating Procedure. Items which may be moved over the storage racks in the expansion modification are the empty new and old storage racks and fuel assemblies with the associated handling tool. The critical load for Load Case 6 will be the fuel assembly with its handling tool.

Response 21: The spent fuel storage racks have been designed and fabricated in accordance with the AISC Specification for the Design, Fabrication and Erection of Structural for Buildings exclusively.

Response 22: The Indian Point High Density Spent Fuel Storage Racks have been designed to meet the requirements for Seismic Category I Structures. Linear seismic analyses have been performed to verify the structural adequacy of the design to withstand the loadings encountered during the severe and extreme enviromental conditions of Operating Basis and Design Basis Earthquakes. Non-linear time history seismic analyses have been performed to evaluate the maximum sliding of the storage racks and to determine the maximum frictional resistance load transmitted by the storage racks to the pool floor liner plate during the Design Basis Earthquake. The details of the linear seismic structural analysis and the non-linear time history seismic analysis for sliding are given below:

Linear Seismic Analysis

For the horizontal and vertical seismic analyses, the following mathematical models were developed:

Mathematical Models:

A 10x10 rack has been analyzed in detail. This rack conservatively represents the controlling structural case since it has the longer beam span and will be loaded by greater seismic loads than the smaller racks. The dynamic (frequency) characteristic of the rack is essentially controlled by the dynamic characteristics of its component 2x2 or 3x2 modular cell units. Although the fundamental frequency of the 3x2 modular cell unit is higher than that of the 2x2 modular cell units, the design seismic spectra is such that the lateral seismic G loading for the 2x2 and 2x3 modular cell units will be essentially similar.

For the horizontal and vertical seismic analyses, a mathematical model was developed to represent the 10x10 rack. This model consists of twenty-five (25) lumped mass cantilever beams (representing twenty-five 2x2 modules) rigidly attached to the rack base structure and attached to each other at the top by spacer bars. Each lumped mass cantilever beam has three masses and has the same dynamic (frequency) characteristics as a 2x2 module. This model is used in calculating the maximum stresses in the rack base structure and the reaction loads and stresses in the rack support feet. The distributed masses corresponding to the fuel assembly storage cells, poison elements and contained plus hydrodynamic mass are lumped at appropriate nodal points. The hydrodynamic mass calculations are based on recommendations given in References 1 and 2. The horizontal and vertical weights are distributed such that the resulting lumped mass multi-degree-of-freedom model best represents the dynamic characteristics of the fuel storage rack. The seismic analyses are performed for the fully loaded racks only since this loading condition results in higher seismic accelerations, higher stresses and reaction loads. The boundary conditions and lumped mass locations for the horizontal and vertical seismic analyses are shown in Figures 1 through 5. In order to determine the maximum seismic response of the storage racks, the racks are conservatively assumed to be pinned (not sliding) to the pool floor at the support feet locations.

---

1. Dong, R. G. "Effective Mass and Damping of Submerged Structures," Lawrence Livermore Laboratory, UCRL-52342, April 1978.

2. Fritz, R. J. "The Effects of Liquids on the Dynamic Motions of Immersed Solids," Journal of Engineering for Industry, Trans. ASME, February 1972.

The eigenvalues (natural frequencies) and the eigenvectors (mode shapes) for each of the natural modes of vibration are calculated by using the Lanczos Modal Extraction Methods. The Seismic Response Analyses are performed by the Response Spectrum Modal Superposition Methods of dynamic analysis, using the applicable Response Spectra Curves. Individual modal response of the system are combined in accordance with Section 1.2.1 of Regulatory Guide 1.92. The maximum response (deflection, acceleration, velocity, shear forces, moments, stresses, reaction loads) of the system for each of the three orthogonal spatial components (two horizontal and one vertical) of an earthquake are combined on a square root of the sums of the squares (SRSS) bases (Regulatory Guide 1.92).

The"rattling"effects of the fuel assembly inside the storage cell are conservatively accounted for by imposing the following assumptions:

1. All storage cells contain the fuel assembly.

2. All fuel assemblies simultaneously impact the storage cells.

3. The effect of fuel assembly impact is a two-fold increase in the seismic inertia loadings produced by the impacting fuel assemblies mass. The use of an impact factor of 2.0 is conservative by comparing the base shear response results of the linear response spectrum modal super position analysis (Reference 3) and the non-linear time history analysis (Reference 4).

4. The impact and seismic inertia loads of the impacting masses are added to the seismic inertia loads of the non-impacting masses. The linear seismic analysis of the fuel storage racks are performed utilizing the STARDYNE computer code (Reference 5).

---

3. Nuclear Energy Services, Inc. Document NES 81A0610, "Structural Analysis Report for the Indian Point Generating Station Unit 2 Fuel Storage Racks," November 1979.

4. Nuclear Energy Services, Inc. "Non-Linear Time History Seismic Sliding Analysis Report for Indian Point Generating Station Unit 2" Document NES 81A0615, Nov. 1979.

5. MRI/STARDYNE 3 - Static and Dynamic Structural Analysis Systems for Scope 3.4 Operating System User's Information Manual, Revision A, Control Data Corporation, August 1976.

Non-Linear Time History Seismic Analysis:

For the non-linear time history seismic analysis of the spent fuel assembly/storage cell structure, a 10x10 storage rack and the stored fuel assemblies have been represented by a two dimensional lumped mass finite element model (Figure 6). The model consists basically of two coincident finite element cantilever beams; one representing the 100 storage cells and the other 100 stored fuel assemblies attached to a "floor" mass by means of a non-linear sliding element.

The fuel element cantilever beam consists of masses lumped at the nodal points interconnected by discrete beam elements. Each lumped mass represents the tributary weight of the fuel element mass. The stiffness characteristics of the beam elements are related to the effective flexural rigidity of the assemblies.

The storage rack cantilever beam similarly consists of lumped masses interconnected by discrete elastic beam elements. Each lumped mass represents the tributory weight of the storage cells, water trapped inside the cells and the virtual water mass to account for the hydrodynamic effects. The stiffness characteristics of the storage rack beam elements are related to the dynamic characteristics (fundamental frequency of vibration) of the storage rack as determined by the Lanczos Modal Extraction method of analysis (Reference 3).

In order to account for fuel assembly impact, adjacent masses of the fuel assembly beam and the storage rack beam are laterally coupled by means of non-linear spring/gap elements. The non-linear spring/gap elements permit the adjacent masses to impact each other whenever the gap closes during a seismic event. The stiffness of the non-linear spring is taken as the stiffness value for each spacer grid. An initial gap of 0.287 inch, reflecting the lateral gap between the fuel assembly and the storage cell wall, is provided. The non-linear spring/gap elements are effective for fuel assembly impact on either side of the storage cell.

The two cantilever beams representing the storage cells and fuel assemblies are attached to the pool floor mass by means of the non-linear sliding element to best represent the rack standing freely on the pool floor. The sliding of the rack is initiated when the lateral force in the sliding element exceeds the frictional resistance force which is equal to the coefficient of friction times the vertical weight of the rack. The effective vertical weight is taken as the vertical bouyant weight of the storage rack less the uplift loads due to the vertical component of the Design Basis Earthquake.

---

3. Ibid.

Since the storage racks with 8x8, 9x8, 9x10, and 8x10 arrays consist of 2x2 modules (9x8 and 9x10 racks have some 2x3 modules as well), their dynamic (frequency) characteristics are essentially similar to the 10x10 storage rack. The lateral seismic inertia load and the frictional resistance load for the 8x8, 9x8, 9x10 and 8x10 storage racks would be proportional to the 10x10 storage rack. The storage rack sliding response, which depends upon the relative magnitude of the lateral seismic load and the frictional resistance load, will therefore be identical for the 10x10, 8x8, 9x8, 9x10 and 8x10 storage racks.

The non-linear time history seismic analysis calculations are performed by means of step-by-step integration technique using the ANSYS computer program (Reference 6).

The seismic analysis of fuel storage racks conforms fully with the requirements of Standard Review Plan 3.7.2.

---

6. Swanson Analysis Inc., "ANSYS - Engineering Analysis System," Revision 3, Update 37J, Boeing Computer Services 6600, January 1977.

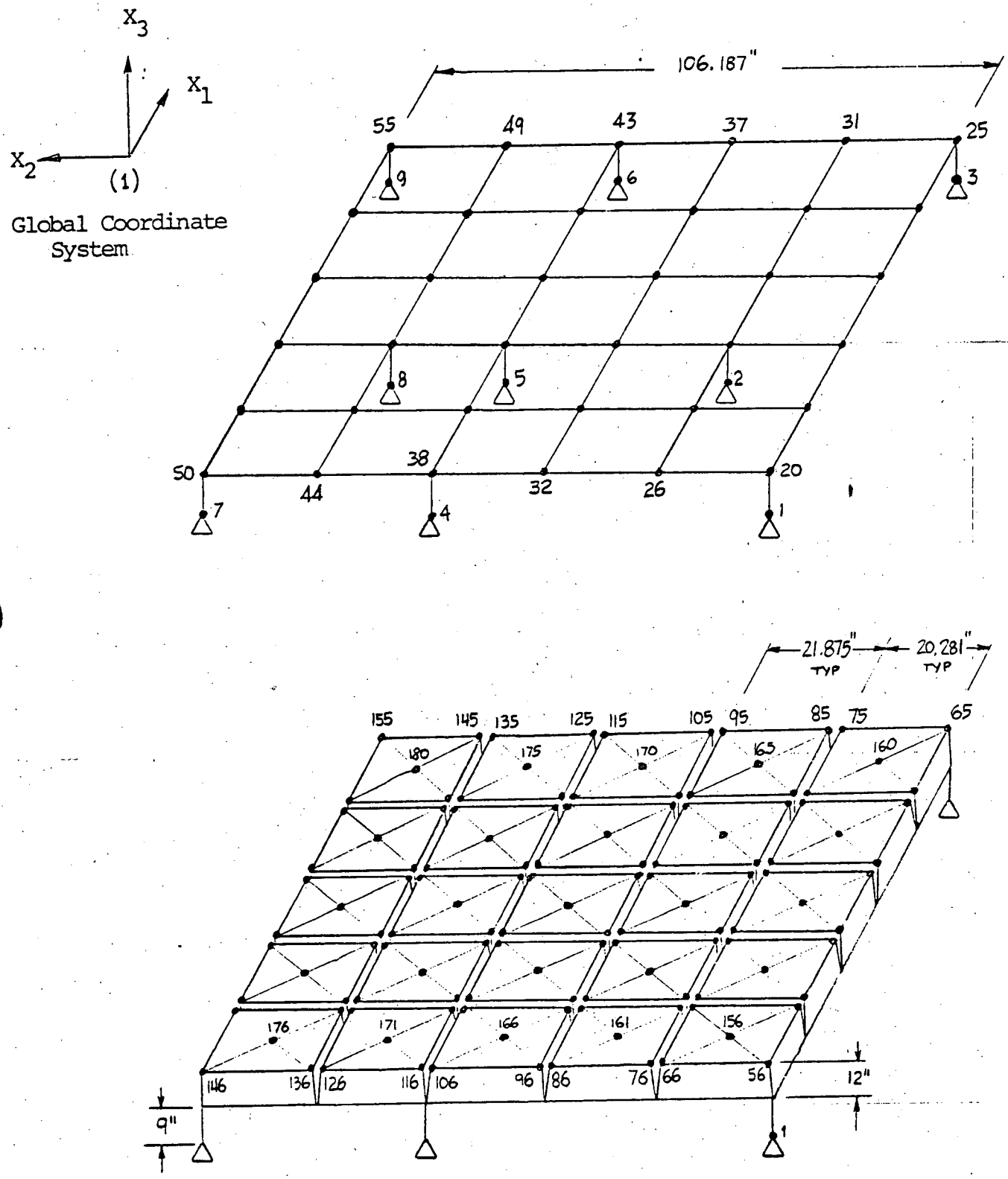

FIGURE 1
10 x 10 RACK FINITE ELEMENT MODEL
DIMENSIONS AND NODE NUMBERS

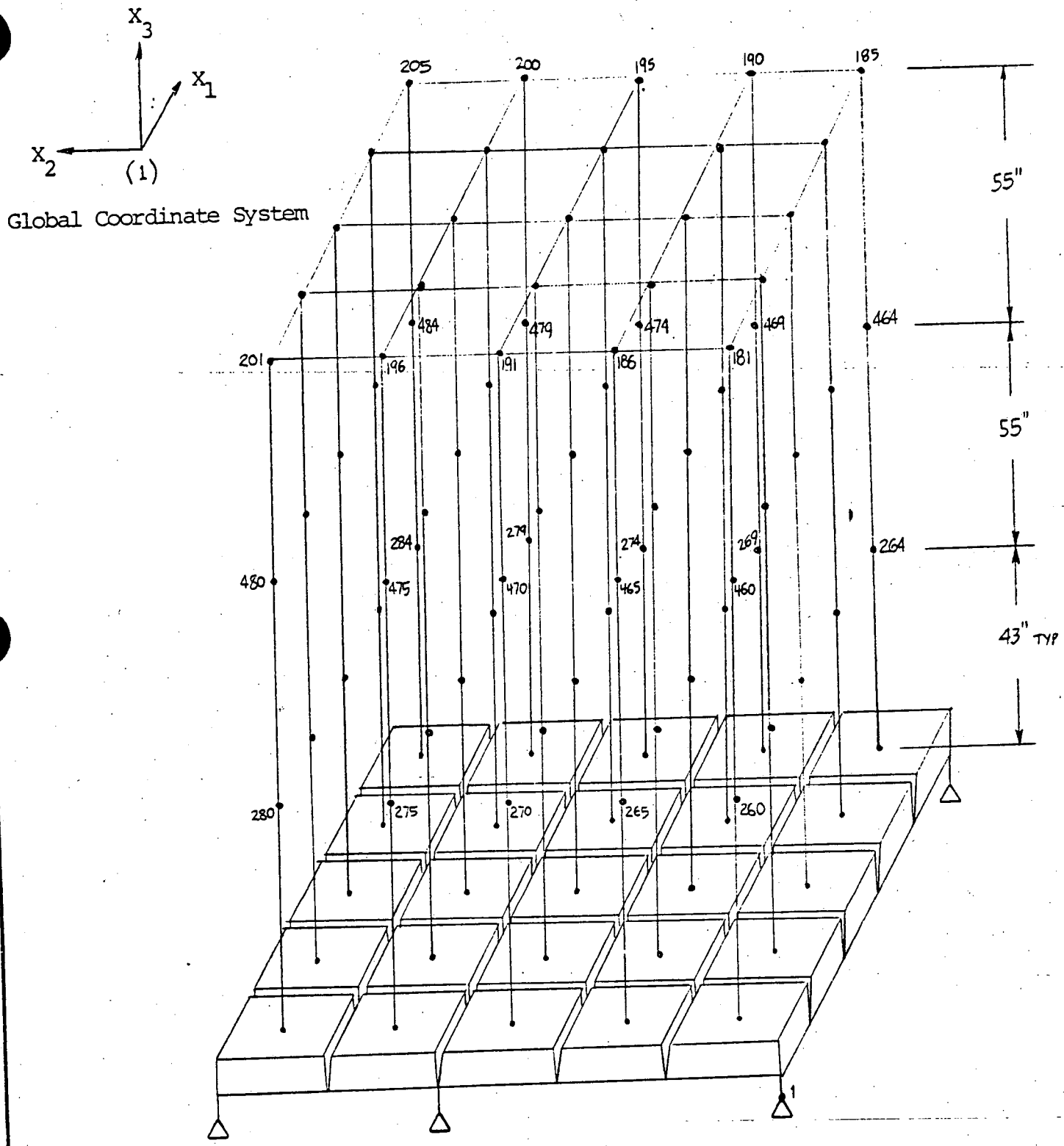

FIGURE 2
10 x 10 RACK FINITE ELEMENT MODEL
DIMENSIONS AND NODE NUMBERS

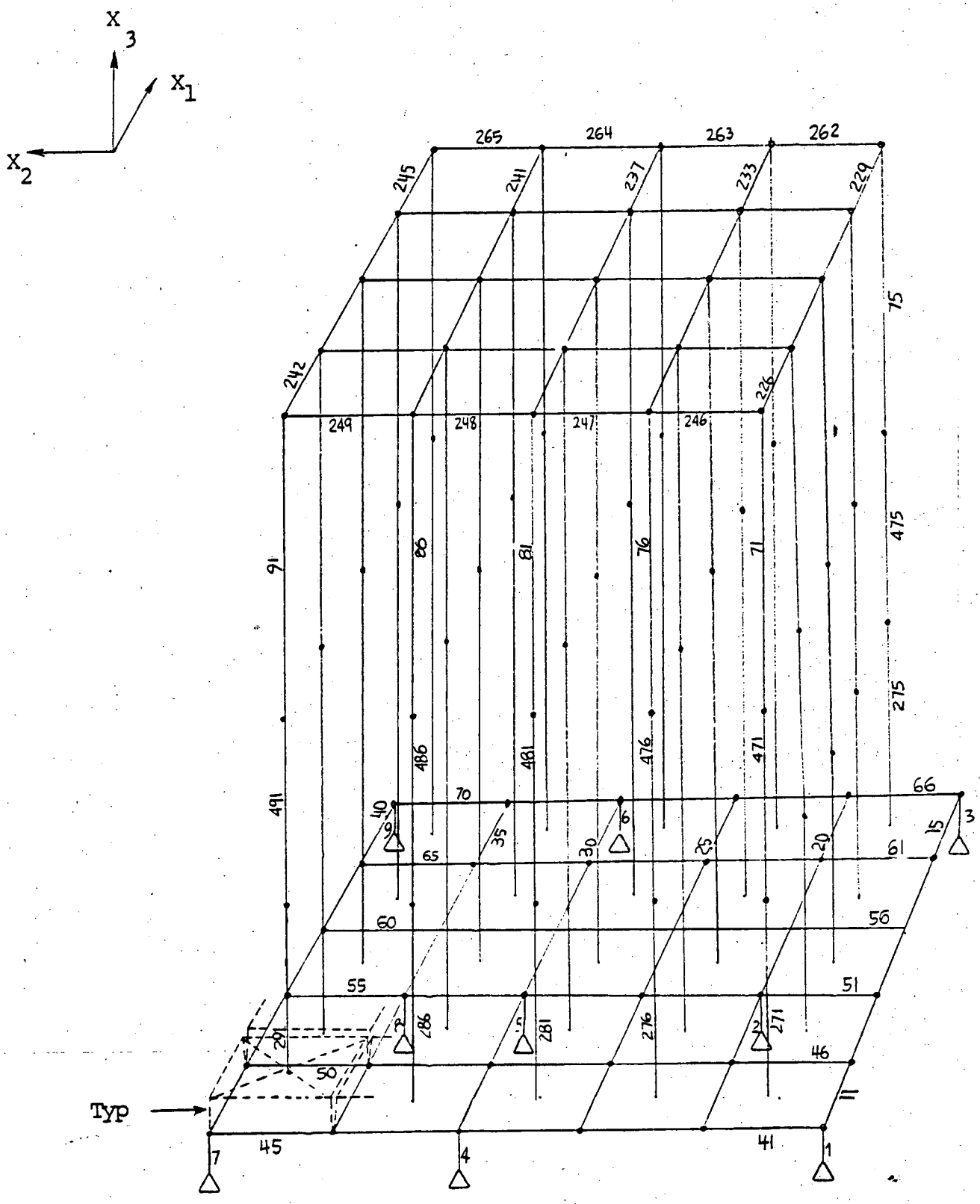

FIGURE 3
10 x 10 RACK FINITE ELEMENT MODEL
BEAM ELEMENT NUMBERS

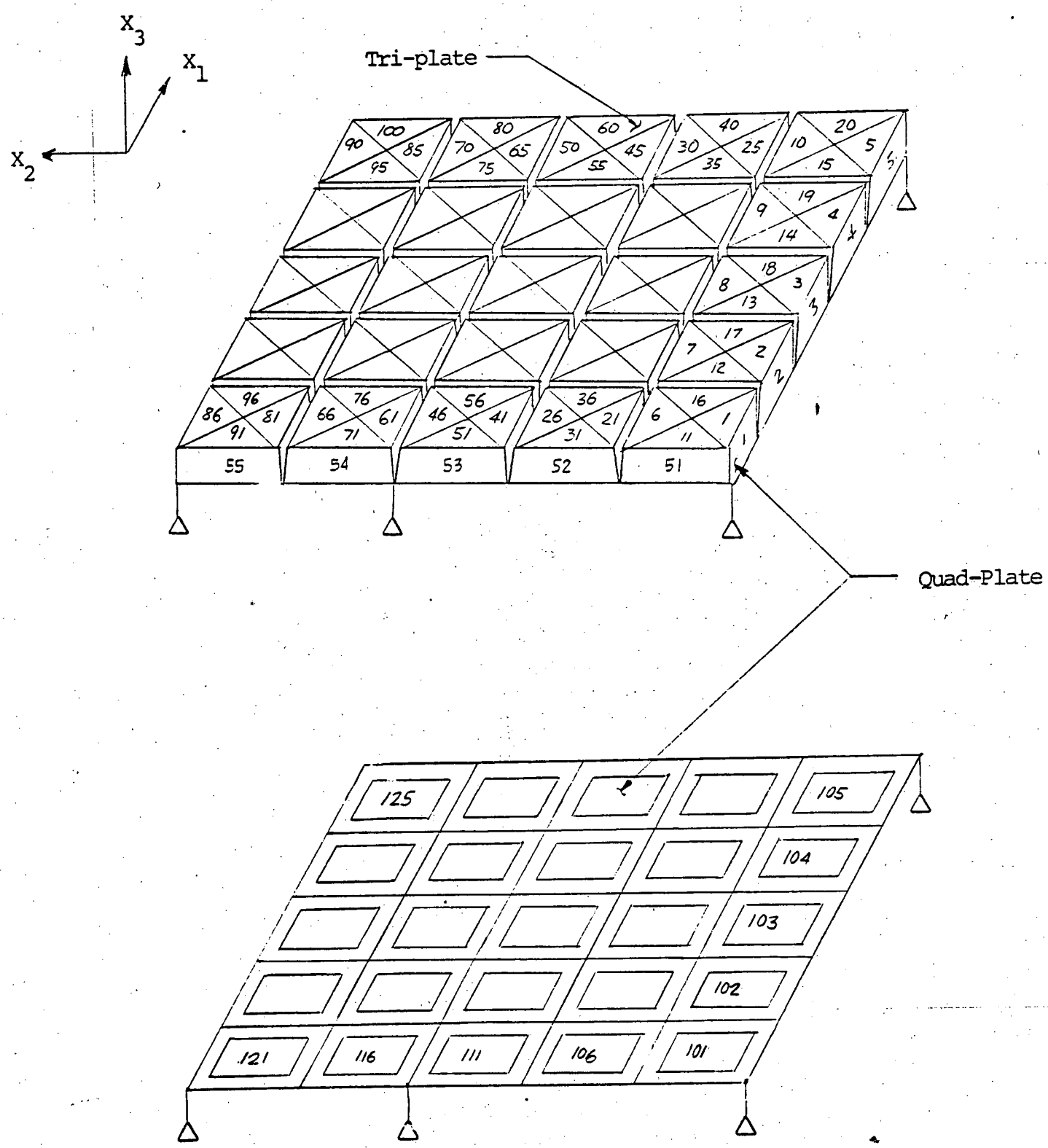

FIGURE 4
10 x 10 RACK FINITE ELEMENT MODEL
PLATE ELEMENT NUMBERS

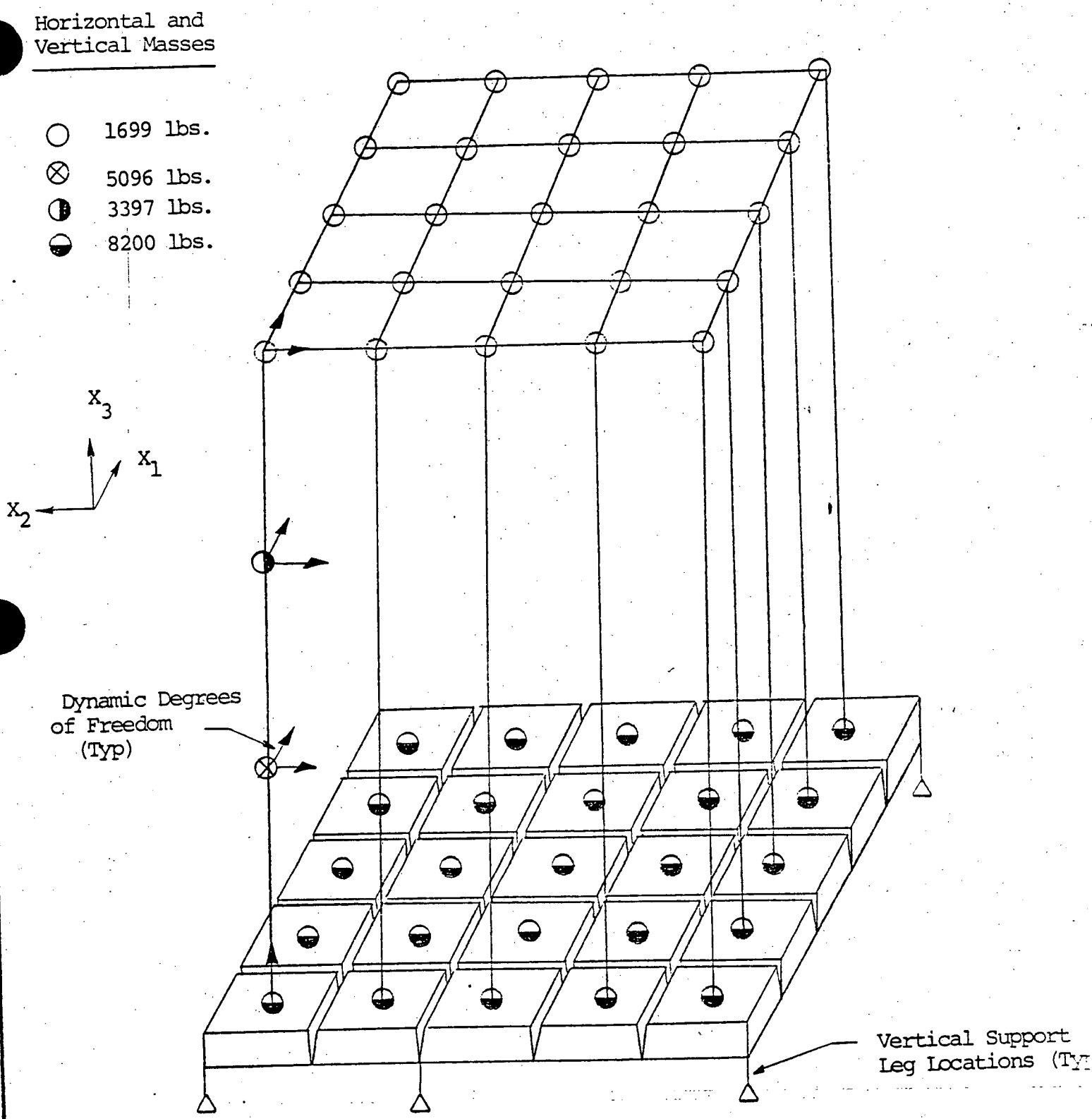

FIGURE 5

LUMPED MASSES AND BOUNDARY CONDITIONS - LOAD CASES 4 & 5
SEISMIC ANALYSIS OF FULLY LOADED 10 x 10 RACK - E AND E'

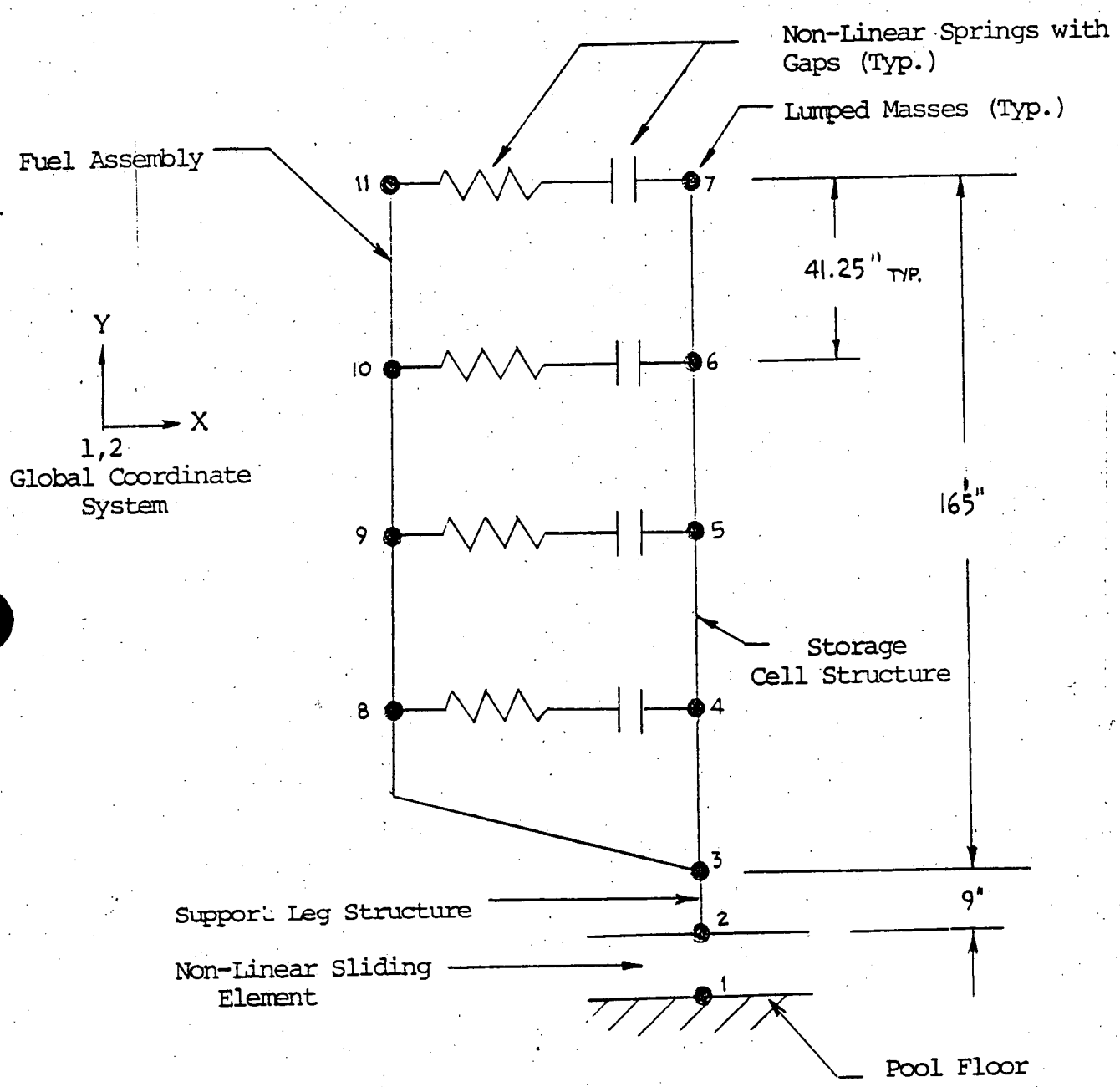

FIGURE 6

Non-Linear Time History Seismic Analysis Lumped Mass Finite Element Non-Linear Model

Response 23: Clearances are provided between fuel assemblies and the storage cells to avoid interferences during fuel storage and removal operations. The storage cell/fuel assembly clearance or gap results in the impacting of the fuel assemby and storage cell during a seismic event. The Indian Point 2 fuel Storage racks have been analyzed using the linear response spectrum nodal superposition methods of dynamic analysis. In these seismic analyses, the effect of impacting masses has been conservatively accounted for by imposing the following assumptions:

1. All storage cells contain the fuel assembly.
2. All fuel assemblies simultaneously impact the storage cells.
3. The effect of fuel assembly impact is a two-fold increase in the seismic inertia loadings produced by the impacting fuel assemblies mass. The use of an impact factor of 2.0 is conservative as verified by comparing the base shear and overturning moment response results of the linear response spectrum nodal superposition analysis

(Reference 1) and the non-linear time history analysis (Reference 2). Attachment I shows the calculation and verification of the impact factors.

4. The impact and seismic inertia loads of the impact masses are added to the seismic inertia load of the non-impacting masses.

1. Nuclear Energy Services, Inc. Document NES 81A0610, "Structural Analysis Report for the Indian Point Generating Station Unit 2 Fuel Energy Racks", November 1979.

2. Nuclear Energy Services, Inc. "Non-Linear Time History Seismic Sliding Analysis Report for Indian Point Generating Station Unit 2" Document NES 81A 0615, Nov. 1979.

ATTACHMENT I

REF.

IMPACT FACTOR TO ACCOUNT FOR THE IMPACT BETWEEN FUEL ASSEMBLY AND STORAGE CELL

GAPS IN THE ORDER OF 0.287 INCHES ARE PROVIDED BETWEEN THE FUEL ASSEMBLY AND STORAGE CELL TO FACILITATE INSERTION AND REMOVAL OF THE FUEL ASSEMBLIES. DURING A SEISMIC EVENT, THESE GAPS ALLOW THE FUEL ASSEMBLY TO RATTLE. TO ACCOUNT FOR THE IMPACT EFFECTS OF THE FUEL ASSEMBLY RATTLING IN THE STRUCTURAL / SEISMIC ANALYSIS, the MAXIMUM STRESSES AND REACTION LOADS DUE TO AN EARTHQUAKE ARE INCREASED BY A DYNAMIC INCREASE IMPACT FACTOR (EFFECTIVE IMPACT FACTORS). The EFFECTIVE IMPACT FACTORS ARE CALCULATED BY APPLYING AN IMPACT FACTOR OF TWO TO the SEISMIC INERTIA LOADS OF THE IMPACTING MASSES

ATTACHMENT I (CONT'D)

REF.

WEIGHT OF FUEL ASSEMBLY = 1.65 k

TOTAL WEIGHT OF FUEL ASSEMBLY, STORAGE CELL AND TRAPPED WATER PLUS HYDRODYNAMIC WATER MASS = 2.50 k

$$\text{Impact Factor} = \frac{2(1.65)+(2.5-1.65)}{2.5} = 1.66$$

VERIFICATION OF THE USE OF AN IMPACT FACTOR OF 2.0:

FOR A 10x10 RACK - DESIGN BASIS EARTHQUAKE EVENT;
MAX. BASE SHEAR FROM THE LINEAR SEISMIC ANALYSIS (TABLE 8.3 OF THIS REPORT 81A0610) = 263.85 K

MAX. HORIZONTAL FRICTIONAL FORCE (BASE SHEAR) FROM NON-LINEAR TIME HISTORY SEISMIC ANALYSIS (TABLE 8.1 OF NES REPORT 81A0615, REF. 13)
= 170.93 K

THE NON-LINEAR TIME HISTORY ANALYSIS MODEL INCLUDED GAP ELEMENTS (IMPACT EFFECTS) BETWEEN THE FUEL ASSEMBLY AND STORAGE CELL. THE LINEAR SEISMIC ANALYSIS INCLUDED AN IMPACT FACTOR OF 2.0. THE BASE SHEAR VALUE (263.85K) FOR THE LINEAR SEISMIC ANALYSIS IS GREATER THAN THAT FOR THE NON-LINEAR TIME HISTORY SEISMIC ANALYSIS, THEREFORE THE USE OF AN IMPACT FACTOR OF 2.0 IS CONSERVATIVE.

Response 24: The free fall of a fuel assembly through the storage cell from a height of 48 inches (Refer to Response 19, the maximum height is 25") above the top of a storage rack and its impact on top of the cell base plate and rack base structure was analyzed using empirical missile equations (the Ballistic Research Laboratory).

The results indicate that the maximum thickness of steel plate that could be perforated by such a missile is slightly greater than the thickness of the cell base plate. Therefore, during a fuel assembly drop accident of this type, the fuel assembly lower end fitting feet would be expected to perforate the cell base plate, however the lower end fitting support plate will prevent further penetration of the fuel assembly and subsequent impact to the pool floor linear plate. The kinetic energy developed during the free fall will be absorbed in punching, bending and shearing of the cell base plate, and the flange of the I-beam under the cell base plate, and the tearing of the welds between the cell base plate and cell wall and cell base plate and I-beam. Since for this fuel assembly drop case, the external energy is absorbed by a combination of the punching, shearing and flexural modes, it is not feasible to calculate the ductility ratio of the lower

end fitting plate and the storage cell base plate. The ductility ratio can be calculated if the energy absorption is by flexural mode only.

Response 25: Since the external kinetic energy and the tributary area impacted by the fuel assembly are same for a 2x2 cell module and a 2x3 cell module, the results of the accidental spent fuel assembly drop analysis presented in Reference [1] (Attachment II) are applicable for both the 2x2 cell module and the 2x3 cell module.

1. Nuclear Energy Services, Inc. Document NES 81A0610, "Structural Analysis Report for the Indian Point Generating Station Unit 2 Fuel Storage Racks," November 1979.

ATTACHMENT II

REF.

ACCIDENTAL SPENT FUEL ASSEMBLY DROP ANALYSIS

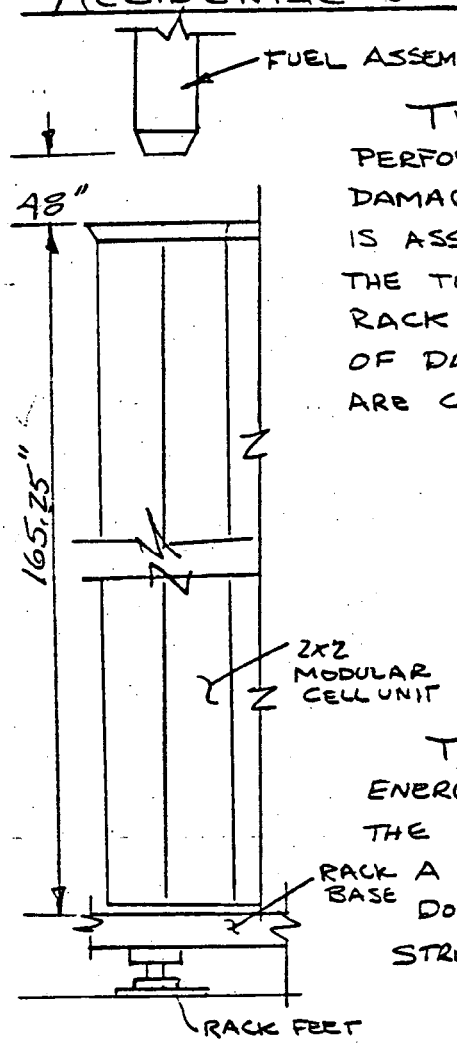

ELEVATION

THE FUEL ASSEMBLY DROP ANALYSIS HAS BEEN PERFORMED TO DETERMINE THE RESULTING STRUCTURAL DAMAGE TO THE STORAGE RACKS. THE FUEL ASSEMBLY IS ASSUMED TO FALL FROM A HEIGHT OF 48.0" ABOVE THE TOP OF THIS STORAGE RACK AND IMPACT THE RACK AT A LOCATION WHERE THE CRITICAL AMOUNT OF DAMAGE WILL RESULT. THREE FUEL DROP CASES ARE CONSIDERED.

1. STRAIGHT DROP ON TOP OF RACK
2. SUBSEQUENT TIPPING ANALYSIS
3. DROP THROUGH STORAGE CELL AND IMPACT AT STORAGE CELL BASE PLATE LOCATION

THIS ANALYSIS CONSERVATIVELY NEGLECTS THE ENERGY LOSSES IN THE LOCAL DEFORMATION OF THE SPENT FUEL ASSEMBLY WHICH RESULTS IN A MORE CONSERVATIVE ANALYSIS OF THE DAMAGE DONE TO THE STORAGE CELLS, AND RACK BASE STRUCTURE.

ATTACHMENT II

REF.

CASE #1 STRAIGHT DROP ON TOP OF RACK

ASSUMING UNIFORM STORAGE CELL COMPRESSION THE EXTERNAL KINETIC ENERGY DEVELOPED IN THE FALL = (FALL HEIGHT) x (WEIGHT OF FUEL ASSEMBLY). NEGLECTING ANY BUOYANT OR DRAG FORCES ON THE FALLING ASSEMBLY –

DROP HEIGHT = 48 INCHES
FUEL ASSEMBLY WEIGHT = 1650 lbs

$$\text{EXTERNAL KINETIC ENERGY} = \frac{48 \times 1650}{1000} = 79.2 \text{ K-IN}$$

THE MAXIMUM REACTION LOADS ARE GENERATED WHEN THE FUEL ASSEMBLY IMPACTS A 2x2 MODULE AT THE INTERSECTION OF THE 4 CELLS (STIFFEST REGION OF TYPICAL 2x2). THE FUEL ASSEMBLY IS ASSUMED TO IMPACT AN AREA EQUIVALENT TO THAT OF A STORAGE CELL, TRANSMITTING AND ABSORBING THE KINETIC ENERGY GENERATED DURING THE FALL. DURING IMPACT, THE LEAD-IN GUIDES WILL COLLAPSE ABSORBING SOME PERCENTAGE OF THE EXTERNAL KINETIC ENERGY. THE STORAGE CELLS ARE EXTREMELY RIGID BECAUSE OF THEIR CONFIGURATION AND THEREFORE IS CONSERVATIVELY ASSUMED TO TRANSMIT THE REACTION LOADS INTO THE YIELDING 2x2 MODULE BASE PLATE.

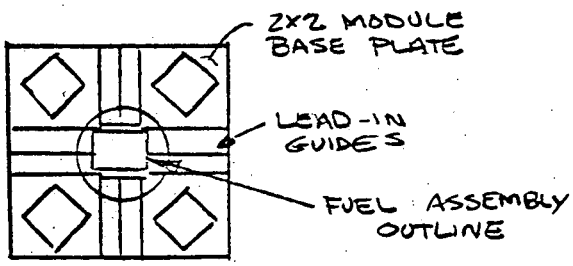

2x2 CELL MODULE PLAN

ATTACHMENT II

REF.

CONSERVATIVELY NEGLECT THE ENERGY LOSSES DUE TO THE LOCAL DEFORMATION OF THE FLARE AT THE TOP OF THE CELL. THE LOCAL DEFORMATION WILL REDUCE THE DAMAGE TO THE CELL; THEREFORE THERE WILL BE LESS DAMAGE TO THE STORED FUEL, AND WILL ALSO REDUCE THE DAMAGE TO THE LINER PLATE AND REINFORCED CONCRETE FLOOR UNDER THE STORAGE CELL.

CALCULATE THE LOAD FROM IMPACT ON THE MODULE.

ASSUME AXIAL COMPRESSION OVER ONE STORAGE MODULE AREA. FIND THE FORCE BY SETTING THE INTERNAL ENERGY ABSORBED EQUAL TO THE EXTERNAL ENERGY OF THE FALLING FUEL ASSEMBLY.

EXTERNAL KINETIC ENERGY OF FUEL ASSEMBLY = 79.2 K·IN

INTERNAL STRAIN ENERGY OF STORAGE CELL (AT 20% STRESS INCREASE) REF. "FINAL STRUCTURAL DESIGN OF A FUEL STORAGE WELL CRASH PAD FOR THE LACBWR NUCLEAR POWER PLANT" Pg. A-18 D.1

$$E_i = \frac{116.9}{1.2} \epsilon_x^{1.20} A \times L \times N$$

WHERE ϵ_x = STRAIN IN STORAGE CELL
A = CROSS-SECTIONAL AREA OF CELL MODULE = 3.26604 IN²
L = LENGTH OF CELL MODULE = 165.25
N = NUMBER OF CELLS = 1.0

$$E_i = E_x$$

$$\epsilon_x = \left[\frac{1.2 E_x}{116.9\ A \cdot L \cdot N}\right]^{1/1.20} = \left[\frac{1.2 \times 79.2}{116.9 \times 3.26604 \times 165.25 \times 1.0}\right]^{1/1.20} = 0.00445 \text{ in/in}$$

CALCULATE % ULTIMATE STRAIN

$$\% \epsilon_u = \frac{\epsilon_x}{\epsilon_u} \times 100 = \frac{0.00445}{0.485} = 0.918\%$$ D.1

MAX DEFORMATION OF THE CELL = δ_x

$$\delta_x = \epsilon_x L = 0.00445 \times 165.25 = 0.735$$

MAX STRESS IN THE CELL

$$\sigma_x = 116.9 \epsilon_x^{0.2} = 116.9 (0.00445)^{0.2} = 39.58 \text{ KSI}$$ D.1 pg A-31

ATTACHMENT II

REF.

USING DYNAMIC YIELD STRESS FOR STAINLESS STEEL = 120% OF YIELD = 1.2(30) = 36.0 KSI FOR 304 SS. F_y = 30 KSI

MAXIMUM TRANSMITTED REACTION LOAD

$$R_x = \sigma_x A = 39.58 \times 3.26604 = 129.27 K$$

CELL BASE PLATE ANALYSIS

THE STORAGE CELL LOADS WILL BE TRANSFERRED INTO THE BASE STRUCTURE THROUGH THE BASE PLATES. THE BASE PLATE WOULD YIELD IF SUCH A LOAD WERE PLACED DIRECTLY ON IT. SINCE THE INDIVIDUAL CELL IS ONLY A PART OF A BUNDLE OF FOUR, ANY FORCE WILL BE DISTRIBUTED THROUGHOUT A MINIMUM OF FOUR CELLS. NEGLECTING ANY ENERGY LOSS DUE TO THE PLATE DEFORMATION, THE IMPACT LOAD WILL BE DISTRIBUTED INTO THE BASE GRID. FROM LOAD CASE 6A AND 6B OF COMPUTER PRINTOUT "JOB007T" THE FOLLOWING STRESSES ARE TAKEN:

MAXIMUM PLATE STRESS = 35.58 KSI

MAXIMUM BEAM BENDING STRESS = 22.92 KSI

THIS LOAD CASE WAS A 189K LOAD PLACED AT THE WORST LOCATION IN ORDER TO FIND MAXIMUM STRESSES. TO FIND THE MAXIMUM STRESSES PROPORTIONAL TO THESE STRESSES.

$$\text{MAX. PLATE STRESS} = \frac{129.27}{189} \times 35.58 = 24.36 \text{ KSI}$$

$$\text{MAX. BEAM BENDING STRESS} = \frac{129.27}{189} \times 22.92 = 15.68 \text{ KSI}$$

THE MAXIMUM LOAD ON A LEG WILL BE TAKEN AS 70% OF THE 129.27 PLUS THE MAXIMUM DEAD + LIVE LOAD CASE LEG FROM COMPUTER PRINTOUT "JOB 007T" LOAD CASE #1 EQUALS 45.16K AT NODE 2.

$$\text{MAX LEG LOAD} = 0.70 \times 129.27 + 45.16 = 135.65^k$$

REF.

ATTACHMENT II

CASE # 2 FUEL ASSEMBLY DROP AND SUBSEQUENT TIPPING

AFTER A FUEL ASSEMBLY IMPACTS THE RACK, IT WILL TIP OVER AND FALL ONTO SEVERAL ADJACENT CELLS. CONSERVATIVELY ASSUME THAT THE FUEL ASSEMBLY WILL FALL DIAGONALLY IMPACTING THE MINIMUM NUMBER OF CELLS.

LENGTH OF FUEL ASSEMBLY = 160 INCHES
NUMBER OF CELLS ON DIAGONAL

$$N = \frac{160}{14.21} = 11.26 > 10$$

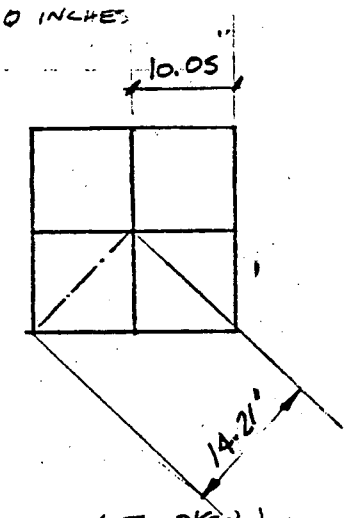

ASSUME 10 CELLS MAX. ARE IMPACTED THEREFORE $\frac{1}{10}$ OF FUEL ASSEMBLY IMPACTS THE 10TH CELL

$$K.E. = \frac{1.65}{10}\left[160 - \frac{160}{10 \times 2}\right] = 25.08 \text{ K-IN}$$

SINCE THE KINETIC ENERGY PER CELL (25.08 K-IN) IS LESS THAN THE KINETIC ENERGY GENERATED IN THE STRAIGHT DROP (79.2 K-IN). THE STRUCTURAL DAMAGE WILL BE LESS SEVERE THAN THE FUEL ASSEMBLY DROP SEE CASE # 1.

REF.

ATTACHMENT II

CASE #3 STRAIGHT DROP THROUGH A STORAGE CELL AND IMPACT A STORAGE CELL BASE PLATE

THE FUEL ASSEMBLY IS ASSUMED TO FALL FROM A HEIGHT 4 FEET ABOVE THE STORAGE RACK, ENTER INTO A SINGLE STORAGE LOCATION AND CONTINUE DOWN THROUGH THE STORAGE CELL IMPACTING THE STORAGE CELL BASE PLATE. THE ANALYSIS CONSERVATIVELY NEGLECTS ANY DRAG OR BUOYANT FORCES ACTING ON THE ASSEMBLY.

MAXIMUM KINETIC ENERGY AT IMPACT $= 1.65(48 + 165.25)$
$= 351.861$ K-IN

MAXIMUM IMPACT VELOCITY $= \sqrt{2gh}$

$$= \sqrt{2 \times 32.17 \times \frac{48+165.25}{12}} = 33.81 \text{ FT/SEC}$$

THE FUEL ASSEMBLY IS ASSUMED TO ACT AS A MISSILE STRIKING THE STAINLESS STEEL BASE PLATE. THE THICKNESS OF PLATE THAT A MISSILE, REPRESENTED BY THE FUEL ASSEMBLY, CAN JUST PERFORATE IS CALCULATED USING THE BALLISTIC RESEARCH LABORATORY (BRL.) EQUATION GIVEN IN REFERENCE D.2

$$T = \frac{\left(\frac{M V_s^2}{2}\right)^{2/3}}{672 D}$$

WHERE: M = MASS OF THE MISSILE $\frac{1650}{32.17} = 51.29 \frac{\text{lb-sec}^2}{\text{FT}}$

T = THICKNESS JUST PERFORATED (IN)

V_s = STRIKING VELOCITY (33.81 FT/SEC)

D = DIAMETER OF MISSILE

CHANGING AREA INTO EQUIVALENT DIAMETER CIRCLE

$$A = 4 \times \left[1.5^2 - \pi \frac{.875^2}{4}\right] = 6.59 \text{ IN}$$

$$D = \sqrt{\frac{4A}{\pi}} = 2.90 \text{ IN}$$

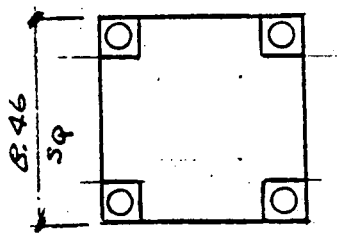

REF.

ATTACHMENT II

$$\text{THICKNESS} = T = \frac{\left[\frac{51.29 \times 33.81^2}{2}\right]^{2/3}}{672 \times 2.90} = 0.489 \text{ IN}$$

RECOMMENDED THICKNESS TO PREVENT PENETRATION = $1.25T = 1.25 \times 0.489 = 0.6113$ IN

CONCLUSION THE FUEL ASSEMBLY WILL PENETRATE THE ½" STORAGE CELL BASE PLATE. ABSORBING A CONSIDERABLE AMOUNT OF THE DROP ENERGY. THE FUEL CELL WILL STOP TO PENETRATE AT THE RETENTION GRID. SINCE THE BASE PLATE IS LOCATED ABOUT 18 INCHES ABOVE THE POOL LINER AND THE END FITTINGS ONLY PROTRUDE 1½" BELOW THE RETENTION GRID, THE POOL LINER WILL NOT BE DAMAGED. SEE SKETCH BELOW.

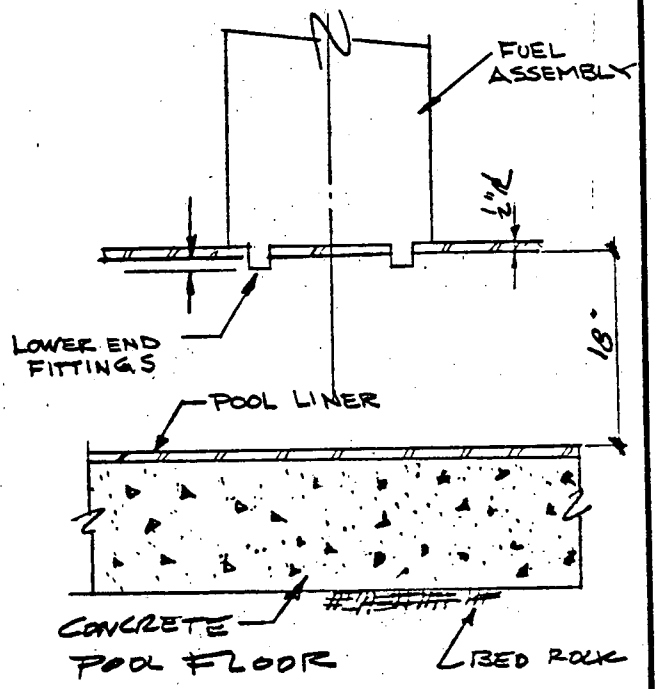

ATTACHMENT II

REF.

THE MAXIMUM REACTION LOAD GENERATED BY THE FUEL ASSEMBLY IMPACT WILL BE ESTIMATED BY CALCULATING THE COLLAPSE LOAD FOR A SQUARE PLATE FIXED AT ALL FOUR EDGES. SINCE THE ACTUAL BASE IS WELDED TO THE BASE BEAM SOME STIFFNESS WILL BE DEVELOPED THRU FLANGE BENDING. BOTH THICKNESS WILL BE USED IN THE CALCULATION, THUS INCREASING THE LEG REACTION.

THE COLLAPSE LOAD MECHANISM FOR A SQUARE PLATE USING AN ANALYTICAL APPROACH IS GIVEN ON PAGE 21 OF REF. #0.3

THE COLLAPSE LOAD $P_c = 6.28(M+m)$

WHERE M = THE POSITIVE MOMENT CARRYING CAPACITY OF THE PLATE PER UNIT LENGTH

$$M = \frac{1 \times t^2}{6} \sigma_y =$$

$$t = 0.375 + 0.5 = 0.875$$

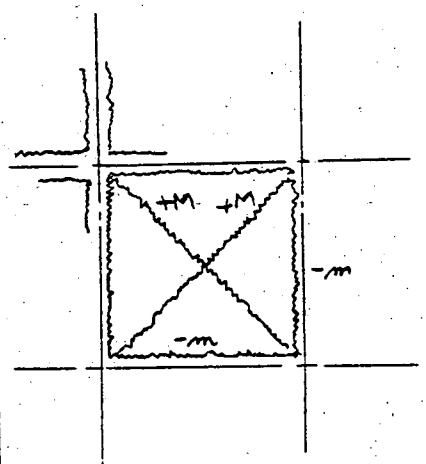

m = THE NEGATIVE MOMENT CARRYING CAPACITY OF THE PLATE PER UNIT LENGTH.

$$m = \frac{1 \times .875^2}{6} \times 1.2 \times 30 = 4.59 \ \frac{K\text{-}IN}{IN}$$

THE YIELD STRESS WILL BE INCREASED BY 20% TO ACCOUNT FOR THE DYNAMIC YIELD $1.2 \times 30 = 36$ KSI

THEREFORE, THE MAXIMUM LOAD THAT CAN BE GENERATED DURING THE FUEL ASSEMBLY DROP EVENT IS:

COLLAPSE LOAD - $P = 6.28(M+m)$

$$P = 6.28(4.59 + 4.59) = 57.65^k$$

MAX TRANSMITTED REACTION = 57.65^k

REF.

ATTACHMENT II

THE REACTION LOAD OF 57.65^k GENERATED DURING THE FUEL ASSEMBLY DROP THROUGH THE CELL AND IMPACT ONTO THE BASE PLATE IS LOWER THAN THAT FOR CASE #1 (PAGE D-3). IT CAN BE CONCLUDED THAT THE EFFECTS ON THE RACK BASE, SUB-BASE MEMBERS, AND RACK SUPPORT LEGS WILL BE LESS SEVERE FOR THE FUEL ASSEMBLY DROP CASE #3 THAN CASE #1 EVEN THOUGH LOCAL DEFORMATION OF THE BASE PLATE WILL BE GREATER.

REF.

ATTACHMENT II

USING MAXIMUM LOAD FROM CASE #1

CALCULATE MAX. STRESS ON POOL LINER AND CONCRETE FLOOR

CHECK BEARING STRESS ON CONCRETE

$$A_p = \frac{\pi D^2}{4} = \frac{\pi(7\frac{1}{2}+\frac{1}{2})^2}{4} = 50.27 \text{ IN}^2$$

$$\text{BEARING STRESS} = \frac{P}{A} = \frac{135.65}{50.27} = 2.70 \text{ KSI}$$

ALLOWABLE BEARING STRESS = $2 \times .85 \phi f'_c$
ACI 318-77 SEC 10.16

$$2 \times .85 \times .7 \times 3.0 = 3.57 \text{ KSI} > 2.70 \text{ KSI}$$

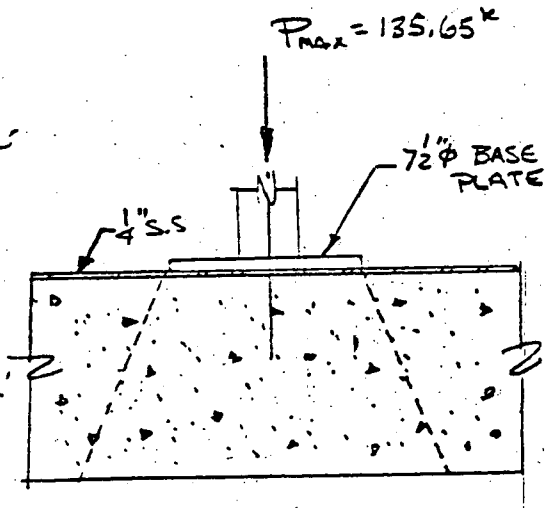

CHECK PUNCHING SHEAR OF POOL LINER

$$\text{SHEAR AREA} = \pi D t = \pi(7.5) \times (\tfrac{1}{4}) = 5.89 \text{ IN}^2$$

$$\text{SHEAR STRESS } f_v = \frac{P}{A} = \frac{135.65}{5.89} = 23.03 \text{ KSI}$$

ALLOWABLE STRESS = 1.2×30 KSI = 36 KSI DYNAMIC YIELD STRESS

CONCLUSIONS

1. ACCIDENTAL DROP OF THE FUEL ASSEMBLY ON THE FUEL STORAGE CELL WILL CAUSE THE FOLLOWING.

   A. THERE WILL BE LOCAL DEFORMATION AT THE TOP OF THE STORAGE CELLS THROUGH LOCAL BUCKLING AND CRUSHING. BUT THE INTEGRITY OF THE RACK BASE SYSTEM WILL NOT BE DAMAGED.

   B. THE LINER PLATE WILL NOT BE PERFORATED, THEREFORE THE LEAK TIGHT INTEGRITY OF THE POOL FLOOR WILL BE MAINTAINED.

ATTACHMENT II

REF.

REFERENCES:

D.1 NUCLEAR ENERGY SERVICES INC, : "FINAL STRUCTURAL DESIGN OF A FUEL STORAGE WELL CRASH PAD FOR LACBWR NUCLEAR POWER PLANT, DOCUMENT NES 81A0426. REV. 1, MARCH 31, 1976.

D.2 LINDERMAN R.B., ROTZ, J.V. AND YEH G.C.K; "DESIGN OF STRUCTURES FOR MISSILE IMPACT," BECHTEL POWER CORPORATION, BC-TOP-9A-REV. 2, SEPT, 1974.

D.3 WOOD, R.H. "PLASTIC AND ELASTIC DESIGN OF SLABS AND PLATES," THE RONALD PRESS COMPANY, N.Y. NY.

Response 26: The fuel storage rack support legs are designed to withstand the maximum horizontal (33 kips) and vertical (107 kips) reaction loads for the dead plus live plus operating basis earthquake event and horizontal and vertical reaction loads of 47 kips and 138 kips respectively for the dead plus live plus design basis earthquake event. The combined effect of the horizontal and vertical reaction loads on the design of the fuel storage rack support leg is considerably greater than that of the vertical reaction load of 136 kips resulting from dead plus live plus fuel assembly drop event.

Response 27: The design load of 3000 lb for the Accidental Uplift Analysis is based on the lifting capacity of the spent fuel handling bridge hoist (2000 lb) and 50% allowance for impact (1000 lb).

Response 28: The non-linear time history seismic analysis has been performed to evaluate the maximum sliding of the storage racks during the Design Basis Earthquake (DBE) event. the results of the analysis are summarized below: The maximum accumulated sliding displacement of the storage rack relative to its initial floor location has been calculated to be 0.125 inches for the coefficient of friction value of 0.20. This maximum displacement value represents the accumulated storage rack sliding response during the ten seconds of the applied time history.

The maximum accumulated sliding displacement value of 0.125 inches is approximately 16.7 percent of the minimum allowable clearance of 0.75 inches available for each rack between the pool walls and their adjacent storage racks base structures, and between rack bases. The maximum rack top deflection was calculated to be 0.697 inches for a coefficient of friction of 1.5, which precludes any sliding between the rack and the pool floor.

The maximum rack cell displacement (rack sliding plus cell top flexural deflection) is therefore 0.822 inch at the flared opening level. This value is approximately 65.8 percent of the minimum available clearance value (1.25 inches) provided for each rack. Therefore, the minimum factor of safety against rack-to-rack or rack-to-wall impact during sliding is 1.52 (1/0.658). The overturning of the fuel storage rack due to Operating Basis Earthquake (OBE) and Design Basis Earthquake (DBE) has been evaluated using energy balance method. The results of the 10x10 spent fuel storage rack stability analysis indicate that:

The storage rack will remain stable during Operating Basis Earthquake (OBE) and Design Basis Earthquake (DBE) events. During OBE event, the storage rack will not be lifted. During DBE event, one edge of the rack will be lifted no more than 0.32 inches.

In order for the storage rack to overturn, its edge would have to be lifted 57.2 inches. Accordingly, substantial margin exists against rack overturning.

Response 29: All spent fuel racks and associated items removed from the spent fuel pool of Indian Point Unit No. 2 must be disposed of by either unrestricted or restricted means. Decontamination procedures will be implemented to attempt to reduce the contamination levels below the maximum level for unrestricted disposal. If successful, there will be no solid radwaste generated by the reracking of Indian Point Unit No. 2

If the decontamination procedures are unsuccessful in reducing the contamination levels sufficiently to allow unrestricted disposal, a maximum volume of 10,500 cubic feet of solid radwaste could be generated by the reracking. This maximum value will be reduced by the implementation of rack disassembly procedures. The extent of volume reduction will depend on contamination and radiation levels and the feasibility of projected cutting techniques. It is believed that the volume could be reduced up to 50% of the maximum volume to about 5000 cubic feet.

Response 30: The Indian Point, Unit 2 spent fuel storage pool cleanup system contains a particulate filter and one 100 gpm mixed-bed demineralizer. There is also a pool surface skimmer with a strainer. We do not expect any impact on the anticipated annual volume of demineralizer resin waste as a result of proposed pool capacity expansion. The reason is that the waste comes mainly from the newly discharged fuel assemblies which have highest activity. The number of fuel assemblies to be discharged during normal operation or abnormal condition are the same for the new rack as for the original rack.

Response 31: (a) Clean waste will be classified as follows: Less than 1000 dpm/100cm^2 loose contamination; and less than 200 cpm fixed contamination (as measured with HP 210 probe).

(b) The collective occupational dose equivalent associated with the spent fuel reracking was estimated for activities given below:

I. Existing rack removal

1. Removal of tie plates
2. Rack removal
3. Pool cleanup

II. Decontamination and Disposal

1. Washing over pool
2. Decontamination
3. Rack cutting and packaging

III. Fuel Movement

IV. New Rack Installation

The estimated total collective occupational dose equivalent for the spent fuel reracking is 25 man-rem. The data used for the derivation are provided below:

Table 1

	Removal and Installation Rack		Fuel Movement*		Decontamination and Disposal Rack	
	Divers	in water support	Gen. Crew	Gen. Crew	Gen. Crew	Total
Manpower	1	2	6	3	4	16
Time (hr_	210	210	420	90	210	
Total (man-hr)	210	420	2520	270	840	
Exposure Rate (mr/hr)	20	1.1	1.1	2.5	20**	
Collective Dose Equivalent (man rem)	4.2	0.5	2.8	.7	16.8	25

*268 assemblies at 20 min/assembly
**This dose rate is based on R.E. Ginna and Donald C. Cook nuclear plant experiences.

(c) The health physics program and the ALARA policy provide for several methods of monitoring.

Before any work is begun, studies will be carried out to determine the effects of fuel distribution in the pool. If substantial dose savings can be realized, spent fuel will be relocated to place the oldest fuel closer to working personnel and the most recently irradiated fuel farther away. Preliminiary calculations have indicated that the exposure rate will decrease by as much as a factor of about 20 with the relocation of fuel.

Before work is begun, measurements of exposure rates will be made both in and around the pool in order to obtain a exposure rate "map" to guide the selection of working times and places. The radiation work permit (RWP) will be based on these calculations and measurements.

Each worker (with the possible exception of those contractors who provide independent monitoring programs) will be equipped with a film badge and a pocket ionization chamber as a minimum. Suitable methods of waterproofing will be provided where appropriate. In addition, extremity monitors (of either film or thermoluminescent types) will be provided to those persons whose work is expected to produce extremity doses more than five times the dose equivalent to the whole body, and the dose to the extremity exceeds 500 mr.

Response 32: Exposure rates near the present spent fuel pool average about 1mR/hr in the truck bay and the cask-washdown pit directly adjacent to the center of the spent fuel array. Survey data shown the primary contribution to the 1mR/hr is probably due to background of that area.

Calculations show that reracking the spent fuel pool cannot raise these exposure rates by more than a factor of 8, even when the new racks become filled. Thus, reracking will add insignificantly to the exposure rate in accessible areas.

Response 33: The location of the area radiation monitor is 5 feet above the catwalk in the north-west corner of the spent fuel pool.

Refer to FSAR pp. 9.5-1 and 11.2-21

Response 34: High and low pool water level is alarmed in the Central Control Room. The high-low alarm is a float switch assembly set for approximately ± 6 inches of normal level.

During the reracking process, the decontamination wash down is the only operation requiring addition of water to the pool. This operation will involve only a limited amount of water, and will be performed under continuous supervision, to insure no over flow from the pool.

Response 35: The maximum rate of heat discharged from the spent fuel pool to the Hudson River occurs when the last batch of fuel assemblies is discharged into the spent fuel pool. Based on the same fuel assembly discharge schedule, the maximum heat discharge rate (in MBtu/hr) will be:

	Original Rack	New Rack	ΔQ	Inc. In Heat Exch. Coolant Outlet Temp. (^{o}F)
Normal Batch Discharge	17.3	18.6	1.3	1.3
Abnormal Full Core Discharge	21.98	24.50	2.52	2.3

Because of the normally large quantity of water from different sources such as circulating water system and service water system for both Indian Point Unt 2 and Unit 3, which are mized at the discharged canal before flowing into the Hudson River, the temperature increase at the river discharge resulting from the additional fuel in the pool is negligible ($< 0.1^{o}F$).

Response 36: Resistance spot welds are being used in the Con Edison spent fuel racks for the assembly of single cells (by joining two angles), for the placement of the poison straps, the 13-inch stiffener plates and the poison bottom retaining plates.

Gas Tungsten Arc Welding and Gas Metal Arc Welding is used for remaining rack fabrication and assembly. NES drawings 80E 3503 Rev 1, 80 E 3505 Rev 3 and 80E 3507 Rev 1 show typical storage rack details. The arc welding procedures and welders are certified in accordance with the requirements of section IX of the ASME B & PV code.

The QA/QC provisions for the spot welding are listed below:

Shop areas used to perform storage cell and module welding were partitioned and enclosed to assure cleanliness. A shop cleanliness program involving the entire nuclear rack fabrication area was in effect to control the amount of airborne dust which can settle on rack components and material. Three semi-automatic welding guns were used in enclosed, limited-access shop areas that were cleaned and vaccumed daily. Pull tests on spot welded test coupons were performed daily at the beginning of each shift and after each shutdown for lunch or for repairs (or regular maintenance, such as change of electrodes). A minimum of six coupons were prepared and tested for each welding machine in operation.

All three machines were used to weld 0.080" to 0.080" sheet metal configuration. One welding gun was also used to join 0.080" to 0.105" sheets (the cell wrapper to 13-inch stiffener and to poison bottom retaining plate). An additional set of six more coupons was tested for this specific configuration as well.

The weld test specimens were machine tested in tension, plugging the welded pieces until fractured, or to the machine limit. No actual fabrication was allowed until all coupons were successfully tested and documented. In addition, 100 percent of the production welds were visually inspected for nugget size, appearance, uniformity, and degree of concavity. Feeler gauges were inserted between the inner surfaces of the two sheets to verify fusion. It is highly unlikely that crater cracking can occur in austenitic stainless steel. Should any weld sample have failed to comply with the acceptance criteria established in the procedure for either the pull test or the visual inspection, machine settings were adjusted in 0.1 second/1 volt increments until twenty consecutive acceptable weld test were obtained. If a specimen fails the tension test, the production of that machine for the previous operating interval is rejected and the welds are remade on the acceptable machine

similarly spaced, but offset from the rejected welds.

The feeding of the materials of the weld guns was performed manually. The material was fixed on a mandrel and clamped to present a uniform geometry. The guns were slung from overhead guide rails. The operator merely placed the gun around the work piece and activated a switch to initiate the welding process. The voltage welding time, and electrode pressure were present and remained fully automatic.

The spacing of the resistance spot welds for the cell assembly was determined to provide an allowable shear strength of 1080 lbs. per weld. The test coupons were required to sustain a minimum tensile strength of 2000 lbs. Documented test results indicate that the process had delivered welds with fracture points between 2800 and 3200 lbs. on a regular basis.

No post weld heat treatment was used in fabricating the racks.

Response 37: The leveling screws are 17-4PH stainless steel in the H 1150 condition. This screw seats in type 304 stainless steel. The anticipated infrequent working of martensitic stainless steel against an austenitic stainless steel does not present a galling problem. A typical installation is shown on NES drawing 80 E 3509 Rev. 0 and 80 E 3519 Rev. 0. The surface

film resulting from the age hardening heat treatment after machining the threads, was removed by grit blasting.